Atmospheric Pollution Research 2 (2011) 300-317

Atmospheric Pollution Research

www.atmospolres.com

Source apportionment of fine particulate matter over the Eastern U.S. Part I: source sensitivity simulations using CMAQ with the Brute Force method

Michael J. Burr, Yang Zhang

Department of Marine, Earth, and Atmospheric Sciences, North Carolina State University, Raleigh, NC, 27695, USA

ABSTRACT

Exposure to elevated levels of fine particulate matter ($PM_{2.5}$) is found to be associated with adverse effects on human health, climate change, and visibility. Identification of major sources contributing to $PM_{2.5}$ is an important step in the formulation of effective reduction strategies. This study uses the U.S. EPA's Community Multiscale Air Quality (CMAQ) modeling system with the brute–force method (BFM) to conduct source apportionment of $PM_{2.5}$ for 10 source categories over the eastern U.S. at a 12 km horizontal grid resolution for both January and July of 2002. Biomass burning is found to be the greatest contributor to domainwide $PM_{2.5}$ with a monthly–mean domainwide contribution of ~14% (1.1 μg m^{-3}). The next two largest contributors in January are miscellaneous area sources and coal combustion with contributions of ~12% (0.9 μg m^{-3}) and ~11% (0.9 μg m^{-3}), respectively. In July, coal combustion, miscellaneous area sources, and industrial processes are the top three contributors (by ~31% (2.3 μg m^{-3}), ~9% (0.7 μg m^{-3}), and ~7% (0.5 μg m^{-3}), respectively). Site–specific source contributions indicate that industrial processes and biomass burning are the most important sources of $PM_{2.5}$ at urban and rural sites, respectively, in January, while coal combustion dominates at both sites in July. While the BFM is theoretically simple and can capture indirect effects resulting from the interactions among precursor and secondary pollutants in the real atmosphere, it is computationally expensive and assumes that the source contributions to each emission category are additive. This assumption does not hold for secondary PM components because of the highly non–linear relationships between precursor emissions and all secondary PM components and, therefore, source apportionment provides no useful information whatsoever on the possible effect of emission reductions on secondary PM.

Keywords:
$PM_{2.5}$
Source apportionment
Brute Force Sensitivity Analysis
CMAQ
Southeastern U.S.

Article History:
Received: 26 September 2010
Revised: 14 January 2011
Accepted: 23 January 2011

Corresponding Author:
Yang Zhang
Tel: +1-919-515-9688
Fax: +1-919-515-7802
E–mail: yang_zhang@ncsu.edu

doi: 10.5094/APR.2011.036

1. Introduction

Particulate matter with an aerodynamic diameter of less than or equal to 2.5 microns ($PM_{2.5}$) is a well researched and documented pollutant due to its adverse health effects and contributions to visibility degradation and climate change. Acute and chronic exposure to elevated levels of $PM_{2.5}$ has been linked to increased mortality rates, heart attacks, decreased lung function, increased asthma attacks, and even premature death (Laden et al., 2000). In December 2006, the U.S. Environmental Protection Agency (EPA) lowered the 24–hour National Ambient Air Quality Standards (NAAQS) for $PM_{2.5}$ from 60 to 35 μg m^{-3}. In order for the state governments to develop the most effective reduction strategies, there must be an understanding of which emission sources are contributing the greatest to $PM_{2.5}$ formation. Source apportionment (SA) is a tool that provides information as to the most important potential sources of $PM_{2.5}$, thus supporting federal, regional, and state agencies in the development of State Implementation Plans (SIPs) and regional and nationwide emission control strategies.

Several different methods of apportioning $PM_{2.5}$ mass to probable emission sources exist, each with their own strengths and limitations, as summarized in Table 1. Receptor–based methods are the most widely–used SA tools that aim to infer contributions from different emission sources using measurements taken at a specific receptor. These methods have been well documented in terms of their mathematical formulation and development (Watson, 1984; Hopke, 1991). Examples of these methods include the chemical mass balance (CMB), positive matrix factorization (PMF), and UNMIX. These methods use a least–squares fitting method in order to minimize the difference between measurements and modeled concentrations. Receptor–based methods are observation–based and are thus generally believed to be reasonably accurate. However, they are limited by the frequency and spatial coverage of observations, problems dealing with co–linearity between source profiles (i.e., sources with similar compositions impacting a receptor site) (Marmur et al., 2005) and secondary pollutants (Seigneur et al., 1999), and in some cases prior knowledge of the composition of emission sources (e.g., CMB) and the need for a very large number of samples (e.g., PMF and UNMIX).

More recent studies have used 3–dimensional air quality models (3–D AQMs) as a source–oriented method for apportioning fine particle mass to potential sources. These emission–based models, as opposed to receptor–based models, use a processed emission inventory as the starting point. While these methods may provide greater spatial resolution than receptor–based models, they are subject to the inherent limitations of the host model and uncertainties in the model inputs used (e.g., dynamic/physical/chemical treatments, emissions, and meteorology).

The simplest SA method using 3–D AQMs is to conduct source sensitivity simulations using the brute force method (BFM), in which a number of sensitivity simulations are performed, each with one source eliminated or reduced and the differences between the results from the sensitivity and baseline simulations are attributed

Table 1. *Summary of existing SA methods that are commonly used*

Type	Example	Strength	Limitation
Receptor-Based	CMB, PMF, UNIMIX	Observation-based Accurate Conceptually Simple	Sparse Observations Some require prior knowledge of emission sources
3-Dimensional *Sensitivity Analysis*	BFM (this study)	Conceptually simple Accurate for linear chemistry and small emission changes Directly related to development of control measures Ability in simulating indirect effects and oxidant-limiting effects	Computationally Expensive Results often non-linear and non-additive Not true "source apportionment" Dependence on baseline Uncertainty in emissions
3-Dimensional *Tagged Species*	PSAT, TSSA	Spatial Distribution Handles non-linearity One model run Variety of "sources" Potential for true source apportionment	Uncertainty in emissions Dependence on baseline simulation Omission of indirect effects and oxidant-limiting effects (for PSAT) assumptions in source apportionment for secondary PM species

CMB: Chemical Mass Balance; PMF: Positive Matrix Factorization; PSAT: Particle Source Apportionment Technology; TSSA: Tagged Species Source Apportionment; BFM: Brute-Force Method; Indirect effects: the reduction of one PM species or PM precursor affecting another through aerosol thermodynamic partitioning processes, gas phase oxidation, and aqueous phase neutralization; Oxidant-limiting effect: the formation of secondary PM species limited by availability of oxidants.

to the source eliminated or reduced. Strictly speaking, the BFM is a source sensitivity (SS) method although it has been used to obtain approximate source contributions through zeroing out emissions from a specific source (e.g., Marmur et al., 2005). A more advanced SS method is to directly calculate the sensitivity coefficients of model outputs to changes in model inputs using a mathematical tool embedded in 3–D models such as the decoupled direct method (DDM) (Dunker, 1984). While these SS methods are a valuable tool for policy–makers to analyze the effects of emission reductions on air quality, they will not provide true SA (i.e., the sum of all source contributions equals the simulated baseline concentrations) if the relationship between the model input and output is non–linear (Yarwood et al., 2005), as is often the case (Hakami et al., 2004). As clearly illustrated in Pun et al. (2008), a reduction in the emissions of secondary PM precursors (e.g., SO_2, NO_x, and VOCs), not only have non–linear effects on their corresponding secondary PM component (i.e., sulfate, nitrate, and organics) but also have non–linear "indirect" effects on the other components that result from interactions between secondary PM species and their gaseous precursors via a number of processes such as aerosol thermodynamic partitioning processes, gas phase oxidation, and aqueous phase neutralization. The BFM catches the indirect effects but reflects the non–linearity only for the perturbation at hand.

More recent studies have implanted a reactive tracer (or tagged species) SA method for $PM_{2.5}$. These tracers are extra species added to a 3–D AQM that track contributions of pollutants from specific source categories and undergo the same atmospheric processes (i.e., dry and wet deposition) within the model as the bulk chemical species (Baker and Timin, 2008). Assuming a pollutant with a total concentration of X with n number of sources, this method assigns a reactive tracer x_i to each source such that the sum of the reactive tracers will equal the total concentration of the species ($X = \sum x_i$). The reactive tracer method differs from the source sensitivity methods in that it has the potential to provide true SA (Yarwood et al., 2005). They, however, are not able to simulate indirect effects and oxidant–limiting effects (i.e., the formation of secondary PM species limited by availability of oxidants) because of some assumptions made in source apportionment for secondary PM species. Examples of such methods include the particle source apportionment technology (PSAT) within the Comprehensive Air Quality Model with Extensions (CAMx) (Wagstrom et al., 2008) and the tagged species source apportionment algorithm (TSSA) within CMAQ (Bhave et al., 2007; Wang et al., 2009).

In this study, two methods are applied to obtain the source contributions of $PM_{2.5}$: the U.S. EPA's Community Multiscale Air Quality (CMAQ) modeling system (Byun and Schere, 2006) with the BFM (referred to as CMAQ/BFM), and the CAMx with the PSAT (referred to as CAMx/PSAT). Our objectives are to estimate source contributions of 10 major source categories to $PM_{2.5}$ over the eastern U.S. using both SS and SA methods, compare simulated source contributions from each method to identify sources of major discrepancies, and make recommendations for their appropriateness for source appointment of $PM_{2.5}$. While there has been extensive research conducted using receptor–based models for $PM_{2.5}$ SA (e.g., Zheng et al., 2002; Marmur et al., 2005), there have been a limited number of SS or SA studies using 3–D AQMs (e.g., Marmur et al., 2005; Bhave et al., 2007; Koo et al., 2009). Different from the most other 3–D studies that focus on one SA method, this study contrasts source contributions of $PM_{2.5}$ using two 3–D AQMs with two most commonly–used SA methods. While a comparison of CAMx/BFM and CAMx/PSAT has been conducted by Koo et al. (2009), this study provides a comparison of BFM and PSAT using two different modeling platforms, allowing for insights into the relative strengths and weaknesses of CMAQ and CAMx in addition to BFM and PSAT.

This work is divided into two parts. Part I presents model evaluation of the baseline simulations using surface observations and source contributions obtained using the CMAQ/BFM for the 10 source categories, including a detailed analysis of monthly–mean source contributions as well as their spatial distributions. Part II presents model evaluation of CAMx/PSAT and SA results obtained for the same 10 source categories using CAMx/PSAT (Burr and Zhang, 2011). The source contributions using the SS and SA methods (i.e., CMAQ/BFM and CAMx/PSAT, respectively) will be compared. The likely causes for their differences as well as the implications of those differences to the SIP modeling and epidemiological studies will be discussed.

2. Methodology

2.1. Baseline simulation

CMAQ version 4.5.1 with a modified secondary organic aerosol (SOA) module by ENVIRON, Inc (Morris et al., 2009) is used to conduct baseline and source sensitivity simulations for 10 source categories over the southeastern U.S. at a 12 km horizontal grid resolution in January and July of 2002. The initial and boundary conditions for both meteorology and chemistry are extracted from a 36 km simulation conducted by the Visibility Improvement State and Tribal Association of the Southeast

(VISTAS) (Morris et al., 2009). CMAQ is configured with 19 layers extending from the surface to the tropopause (~15 km). This study will focus on results in the surface layer (surface to ~38 m) where source apportionment is most relevant. Meteorology is simulated using the Pennsylvania State University (PSU)/National Center for Atmospheric Research (NCAR) 5th generation mesoscale model (MM5) (Grell et al., 1995) version 3.7 with four–dimensional data assimilation (FDDA). The simulation was conducted by Olerud and Sims (2004) in support of VISTAS. The meteorological fields are prepared for CMAQ using the Meteorology–Chemistry Interface Processor (MCIP) version 3.1. The emission inventory used in this research is based on the 1999 National Emissions Inventory version 2 and was provided by Alpine Geophysics, Inc. (Barnard and Sabo, 2008). The emissions are processed using the Sparse Matrix Operator Kernel Emissions (SMOKE) version 2.1 (http://www.smoke–model.org/index.cfm).

2.2. Model evaluation protocol and datasets

The baseline simulation is evaluated against observations in order to assess the uncertainties of the resolved source contributions from the CMAQ/BFM simulations. The variables evaluated include monthly–average concentrations of $PM_{2.5}$ and its individual species [i.e., $PM_{2.5}$, ammonium (NH_4^+), sulfate (SO_4^{2-}), nitrate (NO_3^-), elemental carbon (EC), organic carbon (OC), and total carbon (TC = EC + OC)] as well as maximum 8–h average O_3 mixing ratios. Table S1 in the Supporting Material (SM) summarizes observational datasets for model evaluation. Model evaluation is conducted in terms of spatial distributions and domainwide performance statistics using parameters such as normalized mean bias (NMB), normalized mean error (NME), mean normalized bias (MNB), mean normalized error (MNE), root mean square error (RMSE), and correlation coefficient (COR). Their definitions can be found in Zhang et al. (2006a).

2.3. Design of source sensitivity simulations and procedures for analysis

In this study, source sensitivity simulations with CMAQ/BFM are conducted for 10 source categories in January and July of 2002. Table 2 lists the 10 sources selected based on a literature survey of major sources of $PM_{2.5}$, particularly over the eastern U.S. The sources that are included in the baseline simulations but not in the source sensitivity simulations are offshore and shipping emissions, aircraft emissions, Canadian point sources, and MACT source categories. These uncounted sources will explain unresolved source contributions from the source sensitivity simulations. Emissions are processed separately for each of the 10 source categories, withholding emissions of all species from each source category in one source sensitivity simulation at a time (this method is also referred to as zero–out method, which is a special case of the BFM). Sensitivity simulations are then conducted for each source category using the modified emissions. The difference in simulated species between the baseline and sensitivity simulation is attributed as the contribution of the particular source category. Monthly–mean contributions of each source to the concentrations of $PM_{2.5}$ and its components are calculated as absolute and percentage contributions of each source with respect to the total $PM_{2.5}$ concentrations. In addition, source contributions at representative urban, rural, and coastal sites are analyzed.

3. Model Evaluation

The evaluation of VISTAS's meteorological predictions at 4–36 km in January and July 2002 has been conducted by Olerud and Sims (2004), Olsen (2009), and Liu et al. (2010a). For example, Olsen (2009) reported that MM5 at 12 km underpredicts 2 m temperature by ~15% in January and overpredicts by ~4% in July, and it overpredicts relative humidity at 2 m and wind speed at 10–m, and precipitation by ~11%, ~16%, and ~13%, respectively, in January, and by ~3%, 24%, and ~115%, respectively, in July, over an area in the southeastern U.S. that is a portion of the 12 km domain in this study. The additional evaluation of precipitation simulated by MM5 at 12 km over the eastern U.S. domain in this study shows that precipitation is underpredicted by ~9% in January and overpredicted by ~88% in July. These results, in particular, a large cold bias in 2 m temperature in January and overprediction of precipitation in July, are overall consistent with the current meteorological model performance (Olerud and Sims, 2004).

Table 3, Table S2, and S3 (see the SM) summarize the performance statistics for all surface concentrations for January and July. These results show that the model performs well for O_3 predictions, with NMBs of –8.2% to 7.2% and NMEs from 12.3 – 22.7%. Large biases exist in 24–h average $PM_{2.5}$ concentrations and its components (e.g., overpredicted in January with NMBs of 18.8 – 52.1% but underpredicted in July with NMBs of –39.2% to –26.3% for $PM_{2.5}$). More detailed results along with analysis of likely causes can be found in the SM.

4. Source Apportionment Results

Tables 4 and 5 show the monthly–mean percentage contributions of each source category to the baseline emissions of major species at surface in January and July, respectively. Those in 0–300 m (layers 1–6) are also given for elevated sources from coal combustion. In both January and July, nitrogen oxide (NO_x) emissions are dominated by gasoline and diesel vehicles, with each contributing ~30% in both months. Emissions of volatile organic compounds (VOCs) are dominated by gasoline vehicles and biogenic sources in January with contributions of 29% and 25.7%, respectively. In July, VOC emissions are dominated by biogenic sources that contribute over 70% of the baseline VOC emissions. The largest contributors of sulfur dioxide (SO_2) emissions are coal combustion and other combustion in both months. Other mobile source emissions contribute the greatest to primary $PM_{2.5}$ emissions in both months. Tables 4 and 5 show that the 10 source categories in this study account for greater than 96% of emissions of VOCs, NH_3, and primary $PM_{2.5}$. However, only ~81% of SO_2 is accounted for in both months, and 88.8% and 93.1% of NO_x emissions are accounted for in January and July, respectively. This is attributed to the emissions not considered in the 10 source

Table 2. *Source categories examined in this study*

Source Category	Sources Included
Biogenic	Forests and Vegetation, Wetlands, Wind Erosion, Lightning
Biomass Burning	Wildfires, Prescribed Burning, Agricultural Burning, Residential Wood Burning, Open Burning at Landfills, External Combustion Boilers
Coal Combustion	Electric Generation, Industrial and Commercial External Combustion Boilers; Electric utility, Industrial, Commercial, and Residential Stationary Source Coal Combustion
Diesel Vehicles	On-Road and Off-Road Diesel Powered Vehicles (Emissions from marine vessels and aircrafts excluded)
Gasoline Vehicles	On-Road and Off-Road Gasoline Powered Vehicles (Emissions from marine vessels and aircrafts excluded)
Industrial Processes	Solvent Utilization, Chemical Manufacturing, Food Processing, Metal Production
Miscellaneous Area Sources	Agricultural Production, Animal Waste, Repair Shops
Other Combustion	Natural Gas, Distillate Oil, Residual Oil, Liquefied Petroleum Gas, Compressed Natural Gas, Solid Waste
Other Mobile Sources	Railroads, Aircrafts, Marine Vessels, Road Dust, Pleasure Crafts
Waste Disposal and Treatment	Solid Waste Disposal, Incineration, Site Remediation, Sewage Treatment

Table 3. *Performance statistics for surface and satellite-derived variables simulated by CMAQ in January and July 2002*

		January								
		Mean Obs	**Mean Sim**	**Number**	**NMB**	**NME**	**MNB**	**MNE**	**RMSE**	**COR**
Max 1-h O_3	AIRS-AQS	31.3	32.5	6 191	2.6	19.7	8.9	25.8	8.1	71.9
	CASTNET	33.4	34.9	1 321	4.1	18.7	6.8	19.9	7.5	68.4
	SEARCH	34.4	31.5	62	-8.2	21.6	-5.1	23.2	9.0	64.1
Max 8-h O_3	AIRS-AQS	26.3	28.3	6 189	6.2	22.7	14.2	31.2	7.7	72.3
	CASTNET	30.1	32.1	1 317	7.2	20.5	10.3	23.4	7.6	66.8
	SEARCH	27.7	26.3	31	-5.4	22.3	-1.9	25.1	7.6	74.5
24-h avg. $PM_{2.5}$	IMPROVE	7.7	9.1	292	18.8	38.1	27.8	45.9	4.0	68.5
	SEARCH	10.2	15.6	1 218	52.1	77.3	81.7	101.1	10.5	35.6
	STN	12.9	16.7	518	30.2	48.8	43.4	59.3	9.3	48.2
	AIRS-AQS	13.0	15.1	8 489	16.0	36.3	23.9	41.7	7.2	0.6
		July								
Variable	**Network**	**Mean Obs**	**Mean Sim**	**Number**	**NMB**	**NME**	**MNB**	**MNE**	**RMSE**	**COR**
Max 1-h O_3	AIRS-AQS	65.1	62.0	20 306	-4.7	16.6	0.4	17.9	14.1	76.1
	CASTNET	64.1	59.6	1 349	-7.4	15.3	-3.2	15.4	12.5	77.7
	SEARCH	73.9	71.1	60	-4.2	12.3	-2.7	11.2	10.9	85.4
Max 8-h O_3	AIRS-AQS	57.0	56.6	20 297	-0.7	16.6	5.6	19.5	12.2	76.8
	CASTNET	57.2	55.9	1 341	-2.3	15.3	2.7	16.8	11.1	77.4
	SEARCH	60.3	62.8	57	4.3	13.4	10.4	17.8	11.0	81.6
24-h avg. $PM_{2.5}$	IMPROVE	17.4	10.6	342	-39.2	46.2	-30.1	50.0	10.9	65.5
	SEARCH	19.7	14.5	1 203	-26.3	42.5	-2.0	53.1	11.8	38.1
	STN	21.0	14.7	806	-29.8	47.2	Inf	Inf	14.2	50.7
	AIRS-AQS	20.2	13.9	8 386	-31.4	43.2	Inf	Inf	12.1	60.2

MeanObs: Mean Observed Values (ppb for O_3, μg m^{-3} for $PM_{2.5}$); MeanSim: Mean Simulated Values (ppb for O_3, μg m^{-3} for $PM_{2.5}$); NMB: Normalized Mean Bias; NME: Normalized Mean Error, MNB: Mean Normalized Bias; MNE: Mean Normalized Error, RMSE: Root Mean Square Error; COR: Correlation Coefficient; Inf: Infinity (which occurs when the observed values are extremely small).

categories despite their inclusions in the baseline simulations due to a lack of premerged emission files for those sources (e.g., Canadian point sources, offshore/shipping emissions, aircraft emissions, and maximum achievable control technology (MACT) source categories). These categories account for 19.5% and 18.9% of SO_2 emissions and 11.2% and 6.9% of NO_x emissions in January and July, respectively.

Tables 6 and 7 show the domainwide monthly–mean percentage contributions of each source category to $PM_{2.5}$ and its individual species in January and July, respectively. The corresponding monthly–mean absolute contributions are given in Tables 8 and 9. While positive values indicate that the removal of emissions from a particular source category result in a decrease in the concentration of a particular species (i.e., the positive source contribution of the eliminated source to this species), negative values indicate that the removal of emissions from that source category resulted in an overall increase in that particular species when averaged over the entire domain (i.e., the negative source contribution of the eliminated source to this species). In January, biomass burning contributes the greatest to domainwide $PM_{2.5}$, with a monthly–mean contribution of 13.7% (1.1 μg m^{-3}). Among all species, the contribution of biomass burning to the concentrations of primary organic aerosols is the largest, accounting for 7.4% (0.6 μg m^{-3}) of the overall contribution. Miscellaneous area sources and coal combustion are the other two top source categories, with monthly–mean domainwide contributions of 11.8% (0.9 μg m^{-3}) and 10.8% (0.9 μg m^{-3}), respectively. The domainwide impacts of other mobile sources, industrial processes, and other combustion are comparable in January, with contributions of 6.4% (0.5 μg m^{-3}), 6.4% (0.5 μg m^{-3}), and 5.6% (0.4 μg m^{-3}), respectively. The contributions from other sources are < 4%. In July, coal combustion is the dominant source category, contributing nearly 31% (2.3 μg m^{-3}) of domainwide monthly–mean $PM_{2.5}$, with SO_4^{2-} accounting for nearly 26% (1.9 μg m^{-3}) of the overall contribution. Miscellaneous area sources, industrial processes, and other mobile sources are the next top three source categories with contributions of 8.9% (0.7 μg m^{-3}), 6.9% (0.5 μg m^{-3}), and 4.7% (0.5 μg m^{-3}), respectively. The contributions from other sources are < 3.5%. The impacts of gasoline vehicles are less in July than in January [2.1% (0.2 μg m^{-3}) vs. 3.9% (0.3 μg m^{-3})]. In January, motor vehicle emissions (e.g., NO_x and VOCs) are much higher during a cold–start operation than a fully–warmed, stabilized operation, which leads to higher $PM_{2.5}$ formation. In July, the evaporative losses of emitted species lead to lower $PM_{2.5}$ formation than expected. The simulated contributions from gasoline vehicles reflect different seasonal variations of the motor vehicle emissions. In both January and July, approximately 35% (2.5 μg m^{-3}) of the monthly–mean $PM_{2.5}$ is not accounted for within the 10 source categories. This may indicate the influence of initial and boundary conditions as well as the unresolved sources not considered in the 10 source categories. The impacts of boundary conditions may also provide an indicator on the role of long range transport (LRT) of pollutants from upwind sources into the simulation domain. Westerly flow will enhance the transport of pollutants from the central and western U.S. and thus increase the impacts of boundary conditions.

Table 4. *Monthly-mean percentage contributions of each source category to speciated emissions in January*

Species	**Biogenic**	**Biomass**	**Coal (lyr 1)**	**Coal (lyrs 1-6)[1]**	**Diesel**	**Gasoline**	**Industrial**	**Misc.**	**Other Comb.**	**Other Mob.**	**Waste**	**Total (lyr 1)**
NO_x	2.8	1.4	1.2	5.9	29.4	33.4	0.7	0.0	12.9	6.8	0.2	88.8
VOC	25.7	8.8	0.1	0.0	1.0	29.0	14.8	0.3	1.6	7.9	10.2	99.4
SO_2	0.0	1.2	27.4	50.9	6.7	7.2	1.3	0.0	31.6	4.7	0.4	80.5
NH_3	4.6	3.8	0.1	0.1	0.4	16.2	5.2	67.2	1.3	0.0	0.9	99.7
Primary $PM_{2.5}$	0.7	24.7	4.2	3.9	0.2	1.5	10.6	2.7	6.7	43.5	1.7	96.5

[1] *Approximate height of 1st 6 layers is 300 m.*

Table 5. *Monthly-mean percentage contributions of each source category to speciated emissions in July*

Species	Biogenic	Biomass	Coal (lyr 1)	Coal (lyrs 1-6)[1]	Diesel	Gasoline	Industrial	Misc.	Other Comb.	Other Mob.	Waste	Total (lyr 1)
NO_x	9.1	0.7	1.0	5.9	36.4	27.7	0.8	0.0	6.4	10.8	0.2	93.1
VOC	70.1	0.5	0.0	0.0	0.6	13.4	6.5	0.2	0.3	3.3	4.2	99.1
SO_2	0.0	1.1	27.1	50.9	13.9	9.1	2.7	0	17.8	8.9	0.5	81.1
NH_3	2.2	0.6	0.0	0.1	0.2	9.2	3.3	83.3	0.3	0.0	0.5	99.6
Primary $PM_{2.5}$	0.5	6.2	2.5	3.9	0.1	1.1	20.1	22.8	0.8	41.6	1.3	97.0

[1] *The approximate height of 1st six layers is 300 m.*

Table 6. *Domainwide monthly-mean percentage contributions to the concentrations of $PM_{2.5}$ and its components in January*

Source	NH_4^+	SO_4^{2-}	NO_3^-	EC	POA	SOA	OIN	$PM_{2.5}$
Coal Combustion (lyr 1)	1.57	8.44	-0.26	0.03	0.03	-0.10	1.12	10.82
Coal Combustion (lyrs 1-6)	1.58	8.74	-0.19	0.03	0.03	-0.10	1.15	11.24
Diesel Vehicles	0.17	-0.26	0.80	0.89	0.40	-0.05	0.02	1.97
Biomass Burning	0.39	0.48	0.67	1.16	7.44	0.49	3.06	13.69
Gasoline Vehicles	1.05	-0.21	2.45	0.05	0.29	0.08	0.15	3.86
Industrial Processes	0.63	1.55	0.87	0.04	0.78	0.14	2.38	6.39
Waste Disposal and Treatment	0.05	0.04	0.11	0.02	0.26	-0.01	0.20	0.69
Biogenic	0.27	0.23	0.60	0.01	-0.03	2.70	0.14	3.98
Other Combustion	0.39	1.24	0.62	0.25	2.05	0.04	1.05	5.64
Other Mobile	0.09	0.08	0.24	0.04	0.48	0.06	5.44	6.43
Miscellaneous Area Sources	3.58	0.40	7.45	0.00	0.02	0.01	0.35	11.81
Total (lyr 1)	8.19	11.99	13.55	2.49	11.78	3.36	13.91	65.28

EC: Elemental Carbon; POA: Primary Organic Aerosol; SOA: Secondary Organic Aerosol; OIN: Other Inorganics

Table 7. *Domainwide monthly-mean percentage contributions to the concentrations of $PM_{2.5}$ and its components in July*

Source	NH_4^+	SO_4^{2-}	NO_3^-	EC	POA	SOA	OIN	$PM_{2.5}$
Coal Combustion (lyr 1)	4.00	25.78	0.17	0.02	0.03	0.11	0.66	30.77
Coal Combustion (lyrs 1-6)	3.98	30.03	0.18	0.02	0.03	0.10	0.65	34.99
Diesel Vehicles	0.24	1.02	0.23	1.08	0.45	0.27	0.03	3.32
Biomass Burning	0.07	0.20	0.01	0.22	1.44	0.12	0.79	2.85
Gasoline Vehicles	0.68	0.44	0.22	0.05	0.33	0.24	0.17	2.13
Industrial Processes	0.53	2.90	0.08	0.03	0.58	0.14	2.63	6.89
Waste Disposal and Treatment	0.03	0.03	0.01	0.01	0.18	0.01	0.14	0.41
Biogenic	-0.27	-1.73	-0.16	0.01	0.03	3.42	0.15	1.45
Other Combustion	0.35	2.20	0.09	0.03	0.43	0.13	0.22	3.45
Other Mobile	-0.01	-0.07	0.01	0.03	0.37	0.04	4.37	4.74
Miscellaneous Area Sources	5.37	-0.03	0.71	0.01	0.20	0.01	2.65	8.92
Total (lyr 1)	10.99	30.74	1.37	1.49	4.04	4.49	11.81	64.93

EC: Elemental Carbon; POA: Primary Organic Aerosol; SOA: Secondary Organic Aerosol; OIN: Other Inorganics

Table 8. *Domainwide monthly-mean absolute contributions ($\mu g\ m^{-3}$) to the concentrations of $PM_{2.5}$ and its components from CMAQ/BFM in January*

Source	NH_4^+	SO_4^{2-}	NO_3^-	EC	POA	SOA	OIN	$PM_{2.5}$
Coal Combustion (lyr 1)	0.12	0.66	-0.02	0.00	0.00	-0.01	0.09	0.85
Coal Combustion (lyrs 1-6)	0.12	0.68	-0.01	0.00	0.00	-0.01	0.09	0.88
Diesel Vehicles	0.01	-0.02	0.06	0.07	0.03	0.00	0.00	0.15
Biomass Burning	0.03	0.04	0.05	0.09	0.58	0.04	0.24	1.07
Gasoline Vehicles	0.08	-0.02	0.19	0.00	0.02	0.01	0.01	0.30
Industrial Processes	0.05	0.12	0.07	0.00	0.06	0.01	0.19	0.50
Waste Disposal and Treatment	0.00	0.00	0.01	0.00	0.02	0.00	0.02	0.05
Biogenic	0.02	0.02	0.05	0.00	0.00	0.21	0.01	0.31
Other Combustion	0.03	0.10	0.05	0.02	0.16	0.00	0.08	0.44
Other Mobile	0.01	0.01	0.02	0.00	0.04	0.00	0.43	0.50
Miscellaneous Area Sources	0.28	0.03	0.58	0.00	0.00	0.00	0.03	0.92
Total (lyr 1)	0.64	0.94	1.06	0.19	0.92	0.26	1.09	5.11

EC: Elemental Carbon; POA: Primary Organic Aerosol; SOA: Secondary Organic Aerosol; OIN: Other Inorganics

Table 9. *Domainwide monthly-mean absolute contributions (μg m^{-3}) to the concentrations of $PM_{2.5}$ and its components from CMAQ/BFM in July*

Source	NH_4^+	SO_4^{2-}	NO_3^-	EC	POA	SOA	OIN	$PM_{2.5}$
Coal Combustion (lyr 1)	0.30	1.94	0.01	0.00	0.00	0.01	0.05	2.32
Coal Combustion (lyrs 1-6)	0.30	2.26	0.01	0.00	0.00	0.01	0.05	2.63
Diesel Vehicles	0.02	0.08	0.02	0.08	0.03	0.02	0.00	0.25
Biomass Burning	0.01	0.02	0.00	0.02	0.11	0.01	0.06	0.21
Gasoline Vehicles	0.05	0.03	0.02	0.00	0.02	0.02	0.01	0.16
Industrial Processes	0.04	0.22	0.01	0.00	0.04	0.01	0.20	0.52
Waste Disposal and Treatment	0.00	0.00	0.00	0.00	0.01	0.00	0.01	0.03
Biogenic	-0.02	-0.13	-0.01	0.00	0.00	0.26	0.01	0.11
Other Combustion	0.03	0.17	0.01	0.00	0.03	0.01	0.02	0.26
Other Mobile	0.01	0.03	0.01	0.02	0.05	0.01	0.33	0.46
Miscellaneous Area Sources	0.40	0.00	0.05	0.00	0.02	0.00	0.20	0.67
Total (lyr 1)	0.83	2.35	0.11	0.13	0.33	0.35	0.89	4.99

EC: Elemental Carbon; POA: Primary Organic Aerosol; SOA: Secondary Organic Aerosol; OIN: Other Inorganics

The effects of seasonality are apparent when comparing the contributions in January and July. Coal combustion shows the biggest seasonality, with a contribution of ~31% (2.3 μg m^{-3}) to surface $PM_{2.5}$ concentrations in July, but only ~11% (0.9 μg m^{-3}) in January. This is likely due to excessive use of air conditioners in July. Analysis of speciated contributions shows that the importance of SO_4^{2-} from coal combustion also exhibits a strong seasonality, with a difference of ~15% (1.3 μg m^{-3}) in the contribution between months. This may be due to several reasons, including high temperatures and high photochemical activities that lead to high SO_4^{2-} formation in July and indirect effects in January. The removal of coal combustion emissions in January also leads to an overall increase in the concentration of PM nitrate (NO_3^-) domainwide, as opposed to a slight decrease in July. The reduction of SO_2 emissions from coal combustion makes more oxidants available to oxidize NO_2, leading to increased production of NO_3^-. The increases in the concentration of NO_3^- will somewhat offset the overall $PM_{2.5}$ reductions, thus lowering the overall impact of coal combustion emissions in January. This indirect effect is particularly important in January when colder temperatures favor NO_3^- formation.

The contributions of diesel vehicle emissions to SO_4^{2-} and SOA also show large differences between January and July. As seen in Tables 6 and 7, the impacts of diesel vehicle emissions on SO_4^{2-} differ considerably between months, with a reduction of 1.02% (0.1 μg m^{-3}) in July, but an increase of 0.26% (0.02 μg m^{-3}) in January. The increase of SO_4^{2-} in January illustrates the enhanced effects of indirect effects during winter months. Elimination of diesel vehicle emissions reduces concentrations of NO_x in the atmosphere which can indirectly affect SO_4^{2-} through two different pathways. The first is the increased availability of oxidants and radicals to oxidize SO_2 in the gas phase when NO_x emissions are greatly reduced (despite the reduction of total amount of oxidants and radicals as a result of less NO_x). The second indirect effect occurs in the aqueous–phase production of SO_4^{2-} in cloud droplets. Reductions in emissions of NO_x will reduce the production of nitric acid (HNO_3) that can dissolve effectively in the aqueous–phase under the winter conditions, which will in turn lower the acidity of the aqueous–phase solution. This reduction in acidity will allow for more SO_4^{2-} to enter into the aqueous phase. These indirect effects are found not to be important in July when NO_3^- is not a significant PM component due to the high volatility of HNO_3 under high temperature conditions and insignificant production of nitrate in the aqueous–phase in cloud droplets. The elimination of NO_x emissions from diesel vehicles leads to significantly less oxidants and radicals available for the oxidation of SO_2 due to reduction of O_3 formation, thus decreasing the formation of SO_4^{2-} in July.

The contributions to domainwide $PM_{2.5}$ of biomass burning also show considerable seasonality. In January biomass burning contributes nearly 14% (1.1 μg m^{-3}) of domainwide monthly–mean $PM_{2.5}$, as opposed to only ~3% (0.2 μg m^{-3}) in July. This discrepancy is largely due to differences in emissions of POA, OIN, and EC between the two months, with considerably higher emissions in January. This is likely due to the increased residential wood combustion in January during which emissions of all species from biomass burning are considerably higher than in July (see Tables 4 and 5).

Miscellaneous area sources, comprised predominantly of agricultural emissions, are also a major contributor to domainwide monthly–mean $PM_{2.5}$ concentrations in both months. Compared with July, their contributions are slightly higher in January, due mainly to a much higher contribution to the concentration of NO_3^- as a result of indirect effect mentioned previously. Large reductions in the emissions of ammonia (NH_3) from agricultural activities lead to a decrease in the formation of NH_4^+. This in turn limits the production of ammonium nitrate (NH_4NO_3), leaving more HNO_3 in the gas phase than in the particulate phase. This effect is not nearly as important in July when warm temperatures do not favor NO_3^- formation and the concentrations of NO_3^- are low.

The contributions of biogenic emissions to domainwide monthly–mean $PM_{2.5}$ also show an interesting trend, with a larger overall contribution in January as opposed to July. While the contributions of this source category to SOA are larger due to larger biogenic emissions in July (see Tables 4 and 5), the main reason for the larger contributions to the total concentration of $PM_{2.5}$ in January is the increase in PM SO_4^{2-} that occurs in July as a result of the elimination of biogenic emissions. Emissions from biogenic sources are comprised predominantly of VOCs that rapidly consume radicals and ultimately form SOA. In July, a large reduction in emissions of VOCs from biogenic sources leaves more oxidants available to oxidize SO_2. This results in a considerable increase in SO_4^{2-} (and other secondary PM species) throughout the domain that offsets the decrease in $PM_{2.5}$ due to the elimination of biogenic sources. Such an indirect effect is not as important in January when VOC emissions are lower and colder temperatures and lower availability of OH radicals do not favor SO_4^{2-} formation.

4.1. Spatial distributions of source contributions

Figures 1 and 2 show that coal combustion is a major contributor to surface $PM_{2.5}$ in both months; however, the spatial distribution and magnitude of the contributions differ considerably. In January, the largest percentage reductions in $PM_{2.5}$ occur throughout the Mid–Atlantic States and off the Atlantic coast. In July, almost the entire interior portion of the domain experiences reductions of over 40% resulting from eliminating coal combustion emissions. Both months have the greatest contributions in and around the Ohio River Valley (ORV) region (e.g., Ohio, Indiana, Pennsylvania, Kentucky, Tennessee, West Virginia), though contributions have much greater spatial distribution in July. This is a highly–industrialized area, as 9 of the

country's top 10 power plants in terms of SO_2 emissions reside in this region (EIP, 2007). SO_4^{2-} is the most affected species of coal combustion, contributing well over 78% of the overall $PM_{2.5}$ reduction in most areas. The contributions of coal combustion to each species throughout the 1st 6 layers are shown in Figure 3 in order to assess the importance of elevated releases and plume rise from coal–fired power plants. The spatial distributions of elevated coal combustion contributions vary little in comparison to surface contributions in January, as reflected in Figure 3 and Table 6. However, elevated coal combustion contributions to $PM_{2.5}$ are considerably higher in July in comparison to surface contributions. This increase is caused primarily by increased SO_4^{2-} contributions in the upper layers, indicating the importance of elevated release and plume rise of SO_2 emissions from coal–fired power plants. These effects are not as important in January, likely due to lower mixing depths during the winter months (~350 m in winter vs. ~500 m in summer, Figures not shown). Figures 4 and 5 show the contributions to SO_4^{2-}, NO_3^-, POA, and SOA from coal combustion in January and July. SO_4^{2-} contributions are much higher (84%) in July when warmer temperatures favor SO_4^{2-} formation. In addition, reduction in SO_2 emissions from coal combustion sources in January leads to a fairly significant increase in NO_3^-. The increase is most noticeable in the areas where the largest SO_4^{2-} reductions occur (see Figure 4), indicating that this is a result of indirect effects described previously. The increase in NO_3^- is not seen as extensively in July when oxidant concentrations are higher and warmer temperatures do not favor NO_3^- formation.

The contributions of diesel vehicle emissions are similar between the two months, with the largest impacts occurring over the large urban areas of the domain (e.g., Atlanta, Chicago, Detroit, Raleigh/Durham, and Charlotte). The contributions are slightly greater in July due to higher emissions of SO_2 (as result of a greater operation of coal–fired power plants in summer) leading to larger SO_4^{2-} contributions. Conversely, gasoline vehicle contributions are higher in January, primarily due to higher NO_3^- contributions. The larger NO_3^- contributions in January are attributed to slightly higher emissions of NO_x as well as favorable meteorological conditions for NO_3^- formation.

The contributions to $PM_{2.5}$ from industrial process emissions show similar spatial distributions in both January and July, with the largest contributions occurring in urban areas (e.g., Birmingham, New Orleans, and Chicago). Analysis of speciated contributions shows that SO_4^{2-} is an important species across the southern half of the domain, particularly along the Gulf Coast. Barnard and Sabo (2008) reported that Mississippi and Alabama are the two states with the highest emissions of SO_2 from petroleum processes and related industrial activities in 2002 with total emissions of 15 560 and 22 991 tons per year, respectively; no other state have SO_2 emissions of more than 8 000 tons per year from petroleum–related industrial processes. Additionally, SO_4^{2-} contributions in Mississippi and Alabama are greater in summer when warmer temperatures and greater oxidant concentrations lead to higher SO_4^{2-} formation.

Biomass burning contributions to $PM_{2.5}$ in January are the largest in the southeastern U.S. (e.g., southwest Georgia; Florida panhandle), the western half of North Carolina, and New Orleans, likely due to prescribed burning. Barnard and Sabo (2008) reported that, within the VISTAS domain, agricultural burning and prescribed burning emissions are the highest in FL, land clearing fire emissions are the highest in NC, and wildfire emissions are the highest in GA. POA is the most affected species, displaying a similar trend in the overall $PM_{2.5}$ reductions in both months (see Figure 4). The biggest difference between biomass burning contributions in January (Figure 4) and July (Figure not shown) is the much greater extent of the contributions spatially in January, consistent with the greater spatial distribution of POA emissions in January. This is likely a result of residential wood combustion during the winter months as a means of heating homes. The same major sources (e.g., agricultural burning, land–clearing fires, wildfires, prescribed burning) exist in July over the southeastern U.S. and NC; however, contributions over the northern half of the domain are much smaller in July due to less residential wood combustion.

Waste disposal and treatment contributions are fairly insignificant in most regions in both months, with the exception of an area of 10–15% contributions located in the U.S. Northeast in both months. Tables 6 and 7 show that the contributions of waste disposal emissions are comprised primarily of POA and OIN, indicating a likely combustion source in this region, possibly open burning of waste.

The impacts of biogenic sources are the greatest over the southeastern U.S. in both months. This is an area typically having high VOC emissions, thus leading to high contributions to SOA (see Figure 6). There is, however, a significant discrepancy between the impacts of biogenic sources over the rest of the domain in January and July. Removing biogenic emissions leads to an increase in $PM_{2.5}$ throughout the U.S. Midwest and Northeast in July. Figure 6 shows that removal of biogenic emissions lead to increases in secondary PM species (e.g., NH_4^+, NO_3^-, and SO_4^{2-}) in July, whereas this effect is not observed in January. These negative contributions, which denote increases in these species, illustrate the non–additive limitation for CMAQ/BFM. Larger reductions in VOC emissions in these areas in July relative to January leave more radicals available to oxidize other gaseous precursors to produce higher secondary PM concentrations. The most notable increase occurs for SO_4^{2-}, a particularly important PM species in July.

The contributions of other combustion emissions are greater in January, particularly throughout the Northeast Corridor. Contributions of 15–20% occur over the New Orleans and Miami areas in both months, however, the impacts of other combustion extend much farther north in January. Table 4 shows that higher emissions of all species from other combustion sources are the primary cause of higher contributions in January. Figures 1 and 2 show that the effects of other combustion emissions are more important across the northern half of the domain in January than in July. Higher emissions of primary PM species occur in this region in January, possibly due to an increased use of space heaters and other alternative heating methods during the winter months (Tian et al., 2009).

The contributions of other mobile sources are fairly similar between the two months, with the largest impacts occurring throughout the upper Midwest and Central Plains states, with contributions of 15–40% spanning these regions. Tables 6 and 7 show that other mobile source contributions are comprised predominantly of primary PM species, particularly other inorganic aerosols (OIN), indicating that re–suspended road dust may be a larger contributor in these regions, despite limitations in the current methods in estimating the emissions of re–suspended road dust particles. Other mobile source contributions are slightly higher in January, due mainly to larger contributions from primary PM species. Tables 4 and 5 show that emissions of primary PM species are similar in January and July; therefore, higher contributions to primary PM species in January may be attributed to lower mixing depths during the winter months.

Miscellaneous area source contributions are also significant in both months, with the largest contributions occurring over the eastern North Carolina and the upper Midwest where agricultural activities are high. Both months show significant reductions in NH_4^+, further indicating that miscellaneous area source emissions are dominated by agricultural NH_3 emissions. The main difference between seasonal contributions is different effects of NH_3 emissions on NO_3^- in January and July, as seen in Figures 4 and 5. As mentioned previously, colder temperatures in January favor NO_3^- formation. Reduction of NH_3 emissions in January leads to

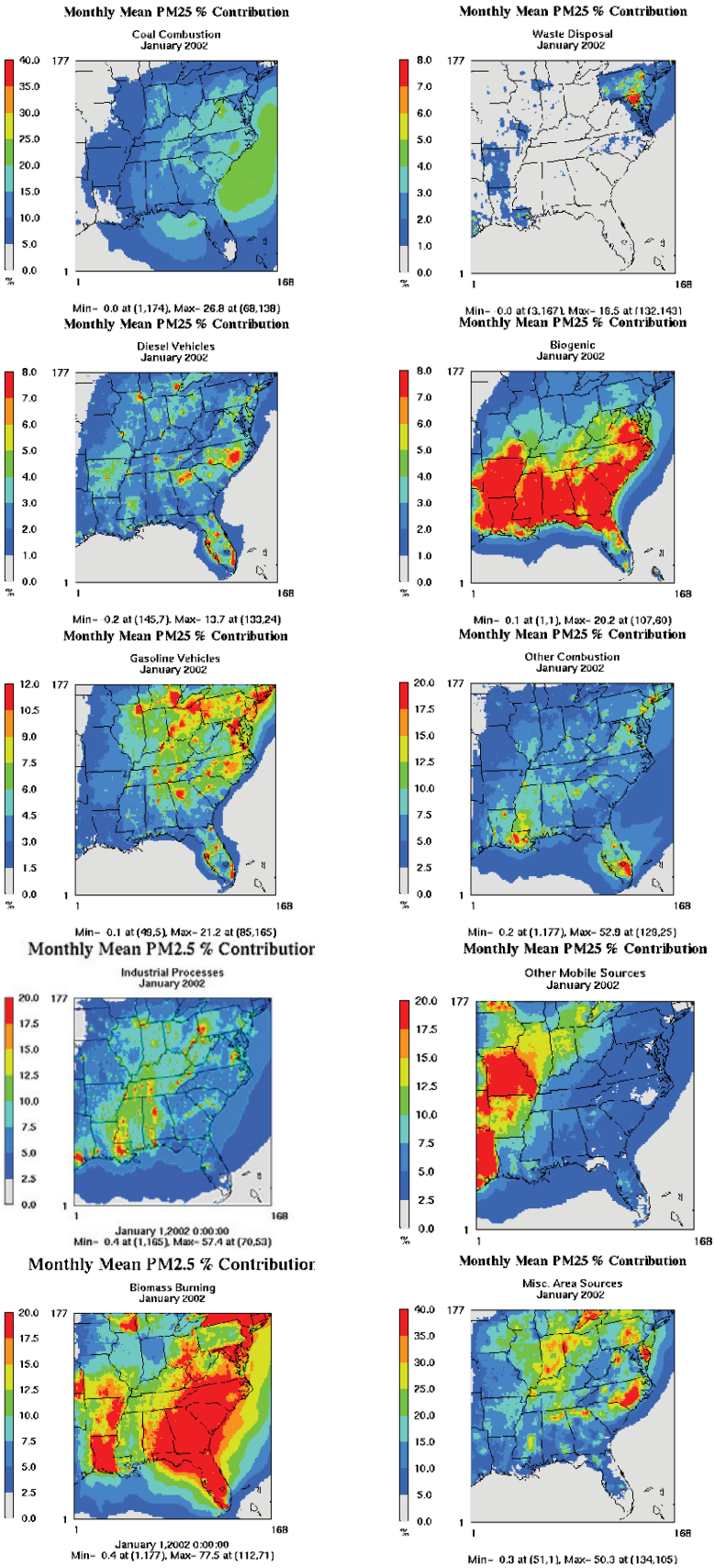

Figure 1. *Spatial distributions of monthly-mean percentage contributions to the concentrations of $PM_{2.5}$ from CMAQ/BFM in January.*

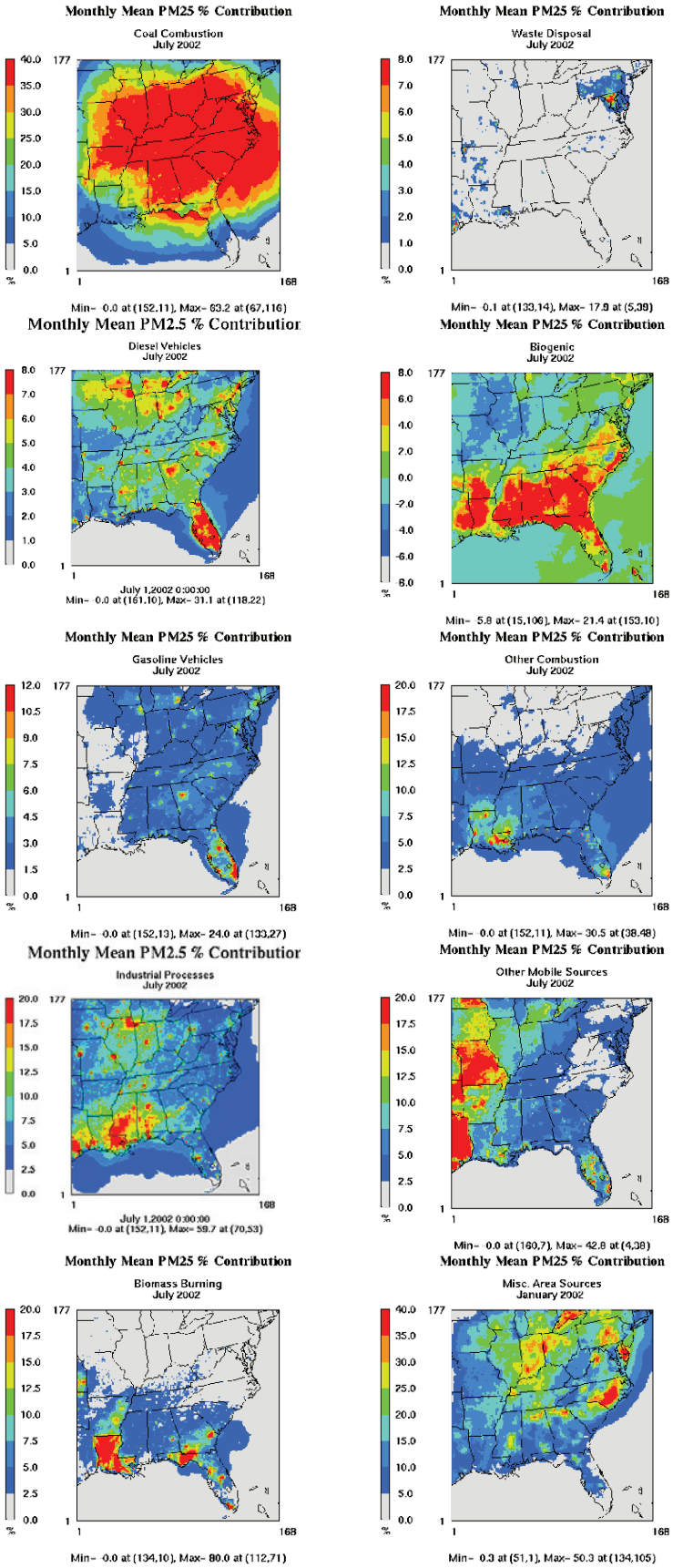

Figure 2. *Spatial distribution of monthly-mean percentage contributions to the concentrations $PM_{2.5}$ from CMAQ/BFM in July.*

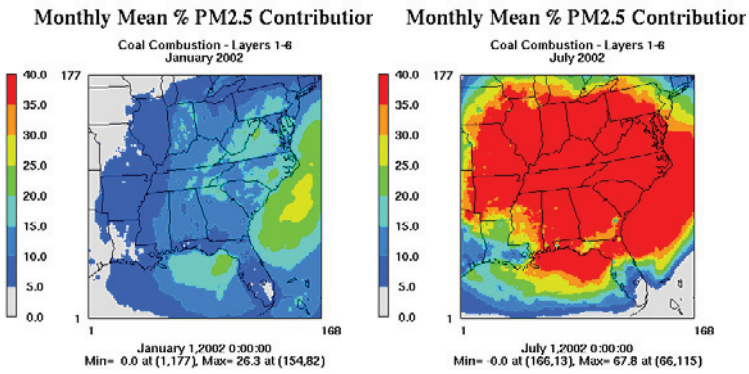

Figure 3. *Spatial distribution of coal combustion contributions to $PM_{2.5}$ in the 1st six layers in January (left) and July (right) from CMAQ/BFM.*

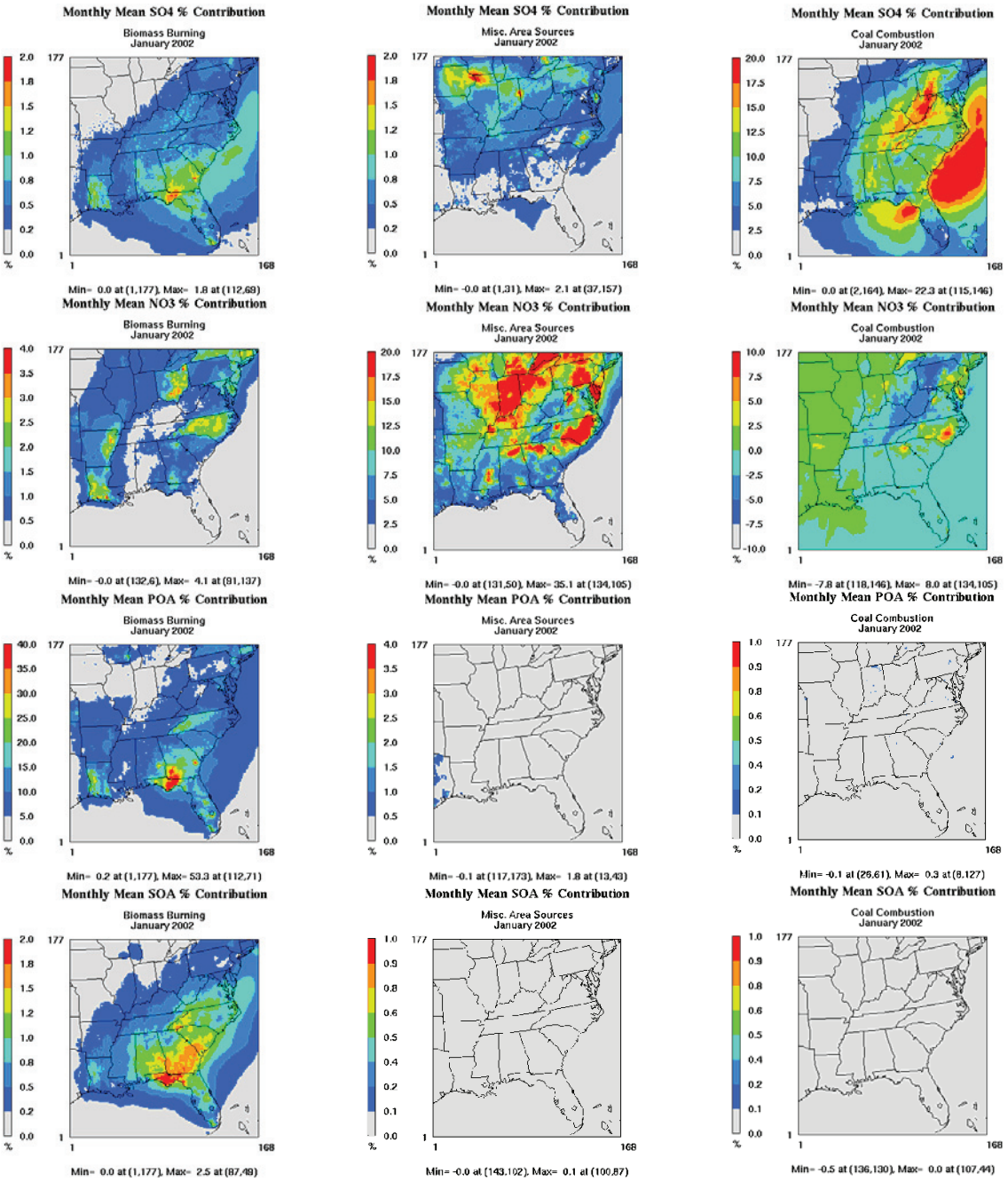

Figure 4. *Contributions of top three source categories (i.e., biomass burning, miscellaneous area sources, and coal combustion) to SO_4^{2-}, NO_3^-, POA, and SOA from CMAQ/BFM in January.*

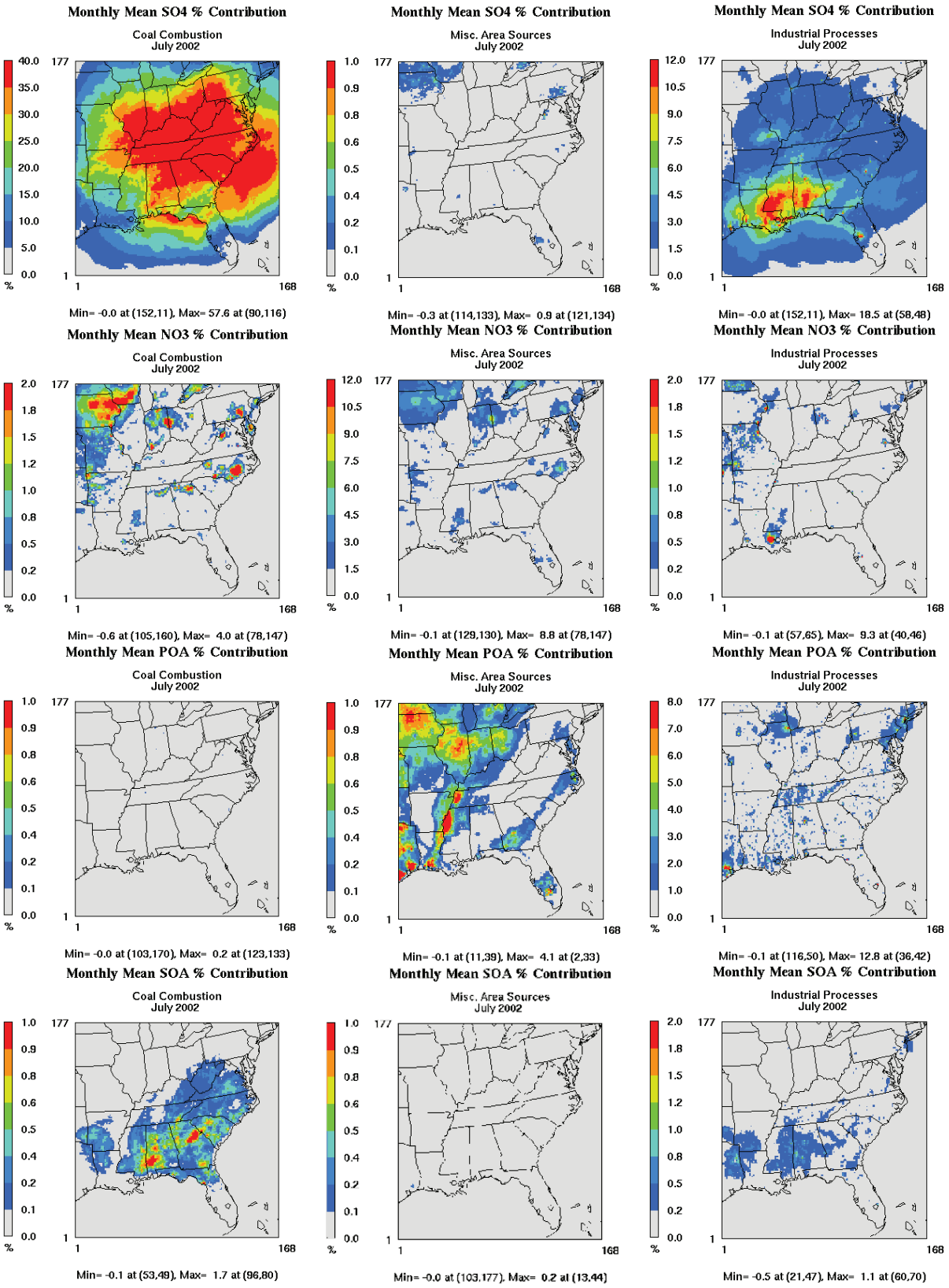

Figure 5. *Contributions of top three source categories (i.e., coal combustion, miscellaneous area sources, and industrial processes) to SO_4^{2-}, NO_3^-, POA, and SOA from CMAQ/BFM in July.*

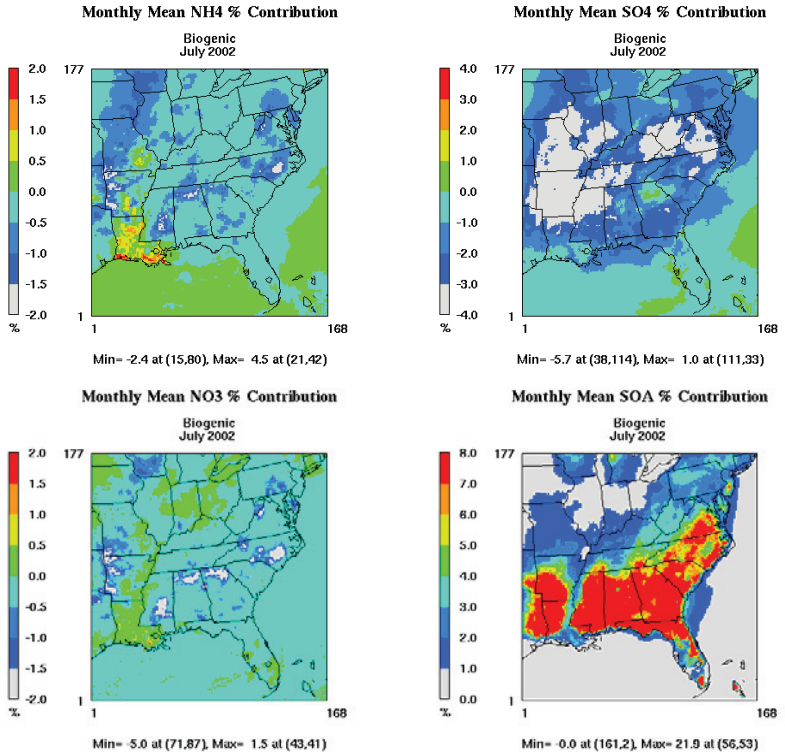

Figure 6. *Impacts of biogenic emissions on the concentrations of secondary PM species from CMAQ/BFM in July.*

less NH_4^+ available to neutralize NO_3^-. As a result, more HNO_3 is left in the gas phase as opposed to partitioning into the particle phase, resulting in a significant reduction in NO_3^- in January, despite insignificant reductions in NO_x emissions (see Table 4). Figure 7 clearly shows that reductions in miscellaneous area source emissions in January lead to an increase in HNO_3 in the same areas where the largest decreases in NO_3^- are observed. This effect is not as important in July when NO_3^- concentrations are not as high due to warmer temperatures. While reductions in NH_4^+ are slightly higher in July as opposed to January, perhaps due to increased animal activities during the summer months, the indirect effects mentioned above are the primary reason for higher contribution from miscellaneous area sources in January.

4.2. Site specific analysis

In addition to the domainwide analysis, source apportionment results at several representative sites throughout the domain are presented in order to analyze how the source apportionment results vary based on the nature of the site (i.e., urban, rural, coastal). These include 8 sites from SEARCH [Jefferson Street (JST), Atlanta, GA, Yorkville (YRK), GA, North Birmingham (BHM), AL, Centreville (CTR), AL, Gulfport (GFP), MS, Grove (OAK), MS, Pensacola (PNS), FL, and Outlying Landing (OLF), FL), 3 sites from AIRS–AQS (Chicago (CHI), IL, Great Smoky National Park (GRM), TN, and New York City (NYC), NY), an urban/rural pair in North Carolina (Charlotte (CLT), NC and Jamesville (JMS), NC), two coastal urban sites (New Orleans (NOR), LA and Norfolk (NFK), VA), and 3 urban sites in the Ohio River Valley [Cincinnati (CIN), OH, Knoxville (KNX), TN, and Nashville (NSH), TN]. These sites represent a mix of urban/suburban, rural, coastal, and park sites that differ considerably in emissions and meteorology. Additionally, source apportionment has been previously conducted in the literature at many of these sites (e.g., Zheng et al., 2002, 2006; Bhave et al., 2007; Ke et al., 2008; Lee et al., 2009) , allowing for qualitative comparisons with this study.

Figure 8 shows averaged source apportionment results at urban, rural, remote, and coastal sites in January and July. The top sources at urban sites are industrial processes (~15%), biomass

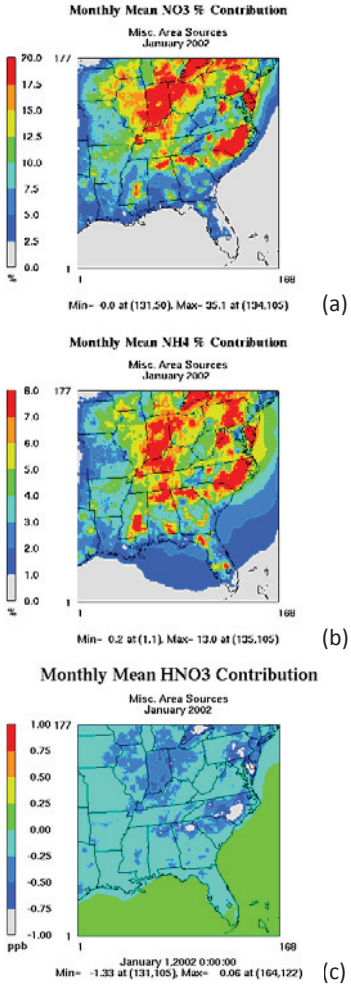

Figure 7. *Miscellaneous area source contributions to the concentrations of NO_3^-* ***(a)****, NH_4^+* ***(b)****, and HNO_3* ***(c)*** *from CMAQ/BFM in January.*

burning (~14%), and other combustion, coal combustion, miscellaneous area sources, and gasoline vehicles (~10–14%) in January. In July, coal combustion (40%) and industrial processes (16%) are dominant sources, and several sources including diesel vehicles, other mobile, miscellaneous area sources, other combustion, and gasoline vehicles also contribute by (~4–6%). At rural sites, major sources include biomass burning (~19%), miscellaneous area sources (~14%), coal combustion (~13%), industrial, biogenic, and other combustion (~9–10%) in January, and are coal combustion (~40%), industrial processes (~10%), and biogenic and miscellaneous area sources (~9%) in July. The top 3 sources at remote sites are biomass burning (~40%), coal combustion (~14%), and miscellaneous area sources (~9%) in January, and are coal combustion (~30%), miscellaneous area sources (~9%), and industrial processes (~6%) in July. At coastal sites, major sources are other combustion (17.3%), miscellaneous area sources, industrial processes, and biomass burning (~12%), and coal combustion and gasoline vehicles (~8–10%) in January, and coal combustion (~24%), industrial processes (~16%), other combustion (~13%), and other mobile sources (~9%) in July.

Differences in the top source categories at various types of sites are apparent when analyzing site–specific percentage contributions in Table 10 and the corresponding absolute contributions in Table 11. For example, the top 3 contributors at JST in January are gasoline vehicles [~21% (3.9 μg m^{-3})], biomass burning [~18% (3.4 μg m^{-3})], and other combustion [~14% (2.6 μg m^{-3})]. Conversely, the top 3 sources at a closely located rural site (YRK) in January are biomass burning [~21% (2.3 μg m^{-3})], miscellaneous area sources [~18% (1.9 μg m^{-3})], and coal combustion [~14% (1.5 μg m^{-3})]. Higher contributions from gasoline vehicles at JST in comparison to YRK can be attributed to heavier vehicle traffic at JST due to a denser population in the urban region. Conversely, higher contributions from miscellaneous area sources at YRK indicate higher agricultural activities at the rural site. Table 4 shows that the majority of NO_x emissions come from diesel and gasoline vehicles as well as other mobile sources. Additionally, the majority of VOC emissions come from biogenic sources and gasoline vehicles. Analysis of site–specific contributions shows that the contributions of diesel vehicles, gasoline vehicles, and other mobile sources are higher at JST than at YRK while biogenic contributions are higher at YRK than at JST. This results in higher NO_x concentrations but lower VOC concentrations at JST while the reverse is true at YRK, attesting VOC–limited O_3 chemistry at JST and NO_x–limited O_3 chemistry at YRK. A similar comparison can be made between co–located urban/rural sites in Mississippi. The top 3 sources at GFP (urban) in July are coal combustion [~21% (1.0 μg m^{-3})], other mobile sources [~14.5% (0.7 μg m^{-3})], and industrial processes [~14.1% (0.7 μg m^{-3})]. Conversely, the top 3 sources at OAK (rural) are coal combustion [~29% (1.7 μg m^{-3})], biogenic sources [20% (1.2 μg m^{-3})], and industrial processes [~11% (0.7 μg m^{-3})]. Higher contributions from industrial processes at the GFP may be attributed to increased activities from various industrial plants (e.g., solvent manufacturing, chemical manufacturing) in this urban region. Higher contributions from biogenic sources at OAK can be attributed to higher biogenic emissions at this rural site as opposed to its urban counterpart. Additionally, the top 3 sources at NYC in January are biomass burning [17.1% (4.9 μg m^{-3})], other combustion [18.8% (5.3 μg m^{-3})], and coal combustion [10.3% (5.0 μg m^{-3})]. The top 3 sources at CHI in January are industrial processes [16.3% (3.0 μg m^{-3})], gasoline vehicles [12.5% (2.3 μg m^{-3})], and other combustion [11.2% (2.0 μg m^{-3})]. As shown in Table 10, the contributions of diesel and gasoline vehicles at NYC and CHI are much larger than the biogenic contributions at these sites in both months, leading to VOC–limited O_3 chemistry at both sites. A similar analysis can be made in determining whether an area is sulfate–rich or sulfate–poor. Tables 4 and 5 show that the dominant sources of NH_3 emissions in both months is miscellaneous area sources. Similarly, the largest source of SO_2 emissions in both months is coal combustion. By analyzing the most important sources at a respective site, we can determine whether the area may be expected to be either sulfate–rich or sulfate–poor. For example, miscellaneous area source

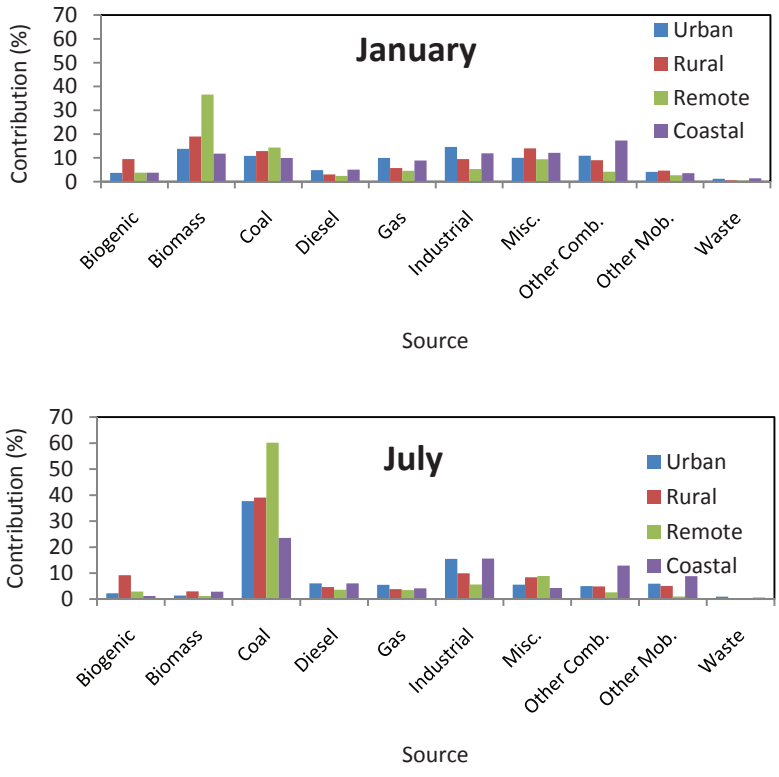

Figure 8. *Monthly-mean percentage contributions to the concentrations of $PM_{2.5}$ at urban, rural, remote, and coastal sites in January (top) and July (bottom) from CMAQ/BFM.*

contributions are much larger [29.3% (3.6 μg m^{-3})] than coal combustion contributions [15.8% (1.6 μg m^{-3})] in January at JMS, likely making the region sulfate–poor. Conversely, coal combustion contributions are large at CLT [14.4% (2.3 μg m^{-3}) in January, 53.2% (7.9 μg m^{-3}) in July] while contributions from miscellaneous area sources are fairly small [10.6% (1.7 μg m^{-3}) in January, 5.8% (0.9 μg m^{-3}) in July], likely making the region sulfate–rich. The top sources at coastal sites are similar to those of urban sites in both months, likely due to the influence of NOR, which is an urban coastal site with large contributions from other combustion [~22% (2.5 μg m^{-3})] and industrial processes [~16% (1.8 μg m^{-3})]. The contributions of waste disposal and treatment and biogenic emissions are fairly small at most sites in both months. Similarly, biomass burning emissions are fairly insignificant at most sites in July while diesel vehicles and other mobile sources are fairly insignificant at most sites in January.

Discrepancies between source contributions at the different types of sites are much smaller in July, with coal combustion having the largest impact at each of the respective group of sites (e.g., urban, rural, coastal, remote). There exist some discrepancies in the contributions of biogenic sources in July, with the largest impacts occurring at rural sites [e.g., by 20.3% (1.2 μg m^{-3}) at OAK and by 11.7% (0.9 μg m^{-3}) at CTR]. Conversely, their co–located urban sites of BHM and GFP have smaller contributions of 4.5% (0.9 μg m^{-3}) and 2.6% (0.4 μg m^{-3}), respectively. The contributions of industrial processes are also shown to be larger at urban and coastal sites than at rural and remote sites in July. This is reflected in Table 10 at BHM, CHI, NOR, and KNX where contribution from industrial processes in July all exceed 20%. Conversely, the largest contributions from industrial processes at rural or remote sites are in the range of 4.4–15.8%. Discrepancies in other source categories (e.g., biomass burning, gasoline vehicles, diesel vehicles, miscellaneous area sources, other combustion, other mobile) are generally smaller in July. This may be due to smaller impacts from indirect effects (e.g., indirect effects of NH_4^+ reduction on NO_3^-) in July as well as differences in emissions (e.g., smaller emissions from biomass burning and other combustion in July) between months.

As mentioned earlier, the "leftover" source category denotes the portion of $PM_{2.5}$ mass that is unexplained by the 10 source categories examined in this study. Large contributions from the leftover source category (> 25%) occur at GFP, OAK, PNS, GRM, NYC, and NFK. OAK, GFP, PNS, and NFK are sites located close to coastlines that are likely influenced more by offshore sources whose emissions are not considered in the 10 source categories. GRM is a national park site with few local sources, and thus may be influenced more by transport from upwind sources. Similarly, studies have shown that a significant portion of $PM_{2.5}$ mass in NYC can be a result of long–range transport (Zhang et al., 2005; Lall and Thurston, 2006). The leftover source category is thus an indicator of the impacts of both long range transport and also sources not considered in the 10 source categories examined in this study.

Also of interest, particularly for source categories whose emissions show considerable daily variation are the weekend versus weekday contributions of source categories. Figure 9 shows the weekend effect of each source category at urban, rural, coastal, and remote sites in January and July. The values are the average contribution of each source during weekends relative to that on weekdays. Therefore, a value of smaller than unity indicates a larger contribution on weekdays relative to weekends. The source showing the greatest overall weekday strength between both months is the diesel vehicle source category, particularly at rural sites in January and at coastal sites in July. Gasoline vehicles show marginal weekday strength at rural and remote sites in January and at coastal sites in July. These are the source categories expected to have the greatest variation between weekdays and weekends due to heavier commuter traffic during the weekdays. The weekday effect is very small at urban sites for diesel and gasoline vehicles, consistent with the finding of Hwang and Hopke (2007), due to little differences in their emissions on weekdays and weekends. The weekend effect of source categories at remote sites show fairly different results in January than in July. In January, biomass burning at remote sites has higher contributions during the weekends, possibly due to differences in emissions and meteorological conditions (e.g., wind speed, precipitation). Conversely, source such at coal combustion, gasoline vehicles, industrial processes, miscellaneous area sources, and other combustion show considerably higher contributions during the weekdays. This may be due to a greater transport of pollutants from urban regions during the weekdays when emissions are higher for some source categories. Conversely, in July, several source categories have higher contributions during the weekends at remote sites (e.g., diesel, gas, other combustion, other mobile, waste disposal and treatment). This may be attributed more to differences in meteorological conditions (e.g., wind speed, precipitation) rather than differences in emissions.

Further considerations should be given to the implications of emissions reductions on ozone (O_3), the other major criteria pollutant with nonattainment issues throughout the U.S. that share the same precursors such as NO_x and VOCs with secondary $PM_{2.5}$. As shown in several studies (e.g., Meng et al., 1997; Pai et al., 2000; Liu et al., 2010b), the emission control strategies that work for O_3 may not work for $PM_{2.5}$ or vice versa. Figure 10 shows the contributions of the 10 source categories examined in this study on monthly–mean maximum 1– and 8–h O_3 concentrations in July. It is found that the elimination of emissions of biogenic source, coal combustion, diesel vehicles, gasoline vehicles, other combustion, other mobile, industrial process can lead to reductions of ~1 to 9% of maximum 1– and 8–h O_3 concentrations domainwide, in particular, the elimination of emissions from biogenic sources, coal combustion, and diesel and gasoline vehicles. These impacts should be taken into account in developing integrated control strategies that are beneficial for both O_3 and $PM_{2.5}$.

5. Conclusions

This study uses CMAQ with the BFM to conduct source apportionment of $PM_{2.5}$ for 10 major source categories for the periods of January and July of 2002. It is found that CMAQ generally overpredicts in January and underpredicts in July the mixing ratios of maximum 8–h O_3 and 24–h $PM_{2.5}$. Possible reasons for biases in simulated O_3 and $PM_{2.5}$ include uncertainties in emissions of precursor species (e.g., SO_2, NH_3, and NO_x), biases in meteorological predictions (e.g, wind speed, precipitation), and uncertainties in their boundary conditions.

Biomass burning is the most important source domainwide in January with a contribution of 13.3% to surface monthly–mean $PM_{2.5}$. POA is the species contributing the largest (7.4%) to the overall $PM_{2.5}$ contribution from biomass burning. Miscellaneous area sources and coal combustion are the 2 next largest sources in January with contributions of 11.8% and 10.8%, respectively. Coal combustion is the most important source domainwide in July, with a contribution of 30.8% to surface monthly–mean $PM_{2.5}$; SO_4^{2-} contributes to 25.8% of the overall $PM_{2.5}$ contribution from coal combustion.Miscellaneous area sources and industrial processes are the 2 next largest sources in July with contributions of 8.9% and 6.9%, respectively. Source contributions are also extracted at 18 representative sites throughout the domain in both January and July. Biomass burning is the most important source at rural sites in January, contributing close to 20% of monthly–mean $PM_{2.5}$. Industrial processes are the most important source at urban sites in January, contributing ~18% of monthly–mean $PM_{2.5}$. Coal combustion is the most important source at both urban and rural

Table 10. *Monthly-mean percentage contributions to the concentrations of $PM_{2.5}$ at representative sites (top 3 sources are highlighted in bold for each month)*

Site	Type	Biogenic		Biomass		Coal		Diesel		Gas		Industrial		Misc.		Other Comb		Other Mob		Waste		Leftover	
		Jan	Jul	Jan	Jul	Jan	Jul	Jan	Jul	Jan	Jul	Jan	Jul	Jan	Jul	Jan	Jul	Jan	Jul	Jan	Jul	Jan	Jul
JST	Urban	4.2	6.4	**17.9**	1.8	12.3	**48.9**	8.0	**8.4**	**20.7**	**10.6**	6.1	6.9	8.5	4.8	**13.8**	5.0	3.0	5.9	1.1	0.9	4.4	0.4
YRK	Rural	7.3	6.3	**21.4**	3.9	**13.7**	**52.9**	3.4	4.7	7.3	4.2	6.9	**6.4**	**17.7**	**11.0**	8.0	4.3	6.3	5.5	0.5	0.3	7.5	0.5
BHM	Urban	4.4	4.5	10.5	1.6	8.9	**29.3**	4.6	5.3	**11.5**	7.2	**29.5**	**35.4**	6.8	2.8	**14.3**	**7.6**	2.7	2.7	1.1	1.0	5.7	2.6
CTR	Rural	**13.1**	**11.7**	**16.1**	3.3	**14.5**	**42.1**	1.9	4.1	3.9	3.2	11.9	**11.8**	9.6	6.5	7.3	5.5	4.7	3.9	0.5	0.2	16.5	7.7
GFP	Urban	5.9	2.6	**10.0**	1.6	8.4	**21.3**	2.6	3.5	4.9	4.0	**9.6**	**14.1**	5.3	2.3	**12.2**	10.6	4.3	**14.5**	0.4	0.3	36.4	25.2
OAK	Rural	**14.4**	**20.3**	**10.7**	2.6	**14.0**	**29.0**	1.8	3.7	2.9	3.0	9.4	**11.3**	8.3	5.1	7.8	6.8	4.7	5.3	0.4	0.3	25.6	12.6
PNS	Urban	3.6	0.0	**14.2**	1.8	**11.1**	**33.9**	1.8	2.6	3.9	2.3	**14.2**	**9.4**	4.5	2.5	8.3	**4.3**	3.4	4.2	0.3	0.1	34.7	38.9
OLF	Rural	4.9	4.4	**24.4**	3.7	6.2	**25.9**	3.5	6.9	6.7	6.3	**12.8**	**15.8**	5.1	4.8	**15.7**	4.2	4.9	**8.8**	0.2	0.1	15.6	19.1
GRM	Park	3.8	2.9	**36.6**	1.2	**14.3**	**30.2**	2.4	3.6	4.6	3.5	5.3	**5.6**	**9.4**	**8.9**	4.2	2.6	2.7	***2.0***	0.4	0.3	16.3	39.2
CLT	Urban	4.9	4.4	**22.7**	1.2	**14.4**	**53.2**	6.4	6.3	**12.8**	**6.6**	6.0	5.4	10.6	5.8	9.2	3.6	3.2	**8.3**	1.9	1.5	7.9	3.7
JMS	Rural	7.8	3.3	**22.1**	1.4	**15.8**	**45.5**	4.4	3.8	7.8	2.4	6.5	**4.4**	**29.3**	**14.6**	6.3	3.6	2.6	***2.0***	1.0	0.5	-3.6	18.5
CHI	Urban	1.6	0.2	6.7	0.2	6.3	**22.7**	7.3	**9.9**	**12.5**	6.7	**16.3**	**23.9**	7.1	5.5	**11.2**	4.7	6.4	6.5	4.5	3.9	20.1	15.8
NYC	Urban	2.1	0.0	**17.1**	0.3	**10.3**	**23.3**	6.2	**10.1**	7.4	6.9	9.1	**9.2**	8.4	6.6	**18.8**	6.6	1.9	2.9	1.4	1.0	17.3	33.1
NOR	Coastal	3.7	2.3	9.3	5.0	5.6	9.0	6.4	7.8	4.7	3.2	**15.7**	**25.2**	**10.3**	3.6	**21.8**	**21.1**	4.8	**11.0**	1.2	0.4	16.5	11.4
CIN	Urban	2.8	0.8	**11.3**	1.0	**13.0**	**51.7**	3.2	4.9	7.8	3.4	9.6	**9.3**	**20.7**	**9.4**	8.2	2.4	7.5	7.2	0.7	0.4	15.2	9.5
KNX	Urban	3.7	2.9	**13.4**	2.9	10.0	**41.9**	3.2	3.2	8.8	3.5	**33.2**	**30.6**	**10.7**	**6.2**	4.8	1.9	3.1	3.2	0.3	0.2	8.8	3.5
NFK	Coastal	3.9	0.1	**14.3**	0.7	**14.3**	**38.1**	3.7	4.3	13.1	5.1	8.1	**6.0**	**13.9**	5.0	12.8	4.7	2.4	**6.7**	1.6	0.8	11.3	28.5
NSH	Urban	3.7	0.3	**14.2**	4.4	**13.7**	**50.8**	5.3	6.3	9.2	4.1	12.1	**10.8**	**17.6**	**9.6**	8.3	3.5	5.4	4.0	0.5	0.2	10.0	6

JST: Jefferson Street (Atlanta), GA; YRK: Yorkville, GA; BHML Birmingham, AL; CTR: Centreville, AL; GFP: Gulfport, MS; OAK: Oak Grove, MS; PNS: Pensacola, FL; OLF: Outlying Landing, FL; GRM: Great Smoky Mountain National Park, TN; CLT: Charlotte, NC; JMS: Jamesville, NC; CHI: Chicago, IL; NYC: New York City, NY; NOR: New Orleans, LA; CIN: Cincinnati, OH; KNX: Knoxville, TN; NFK: Norfolk, VA; NSH: Nashville, TN.

Table 11. *Monthly-mean absolute contributions (μg m^{-3}) to the concentrations of $PM_{2.5}$ at representative sites (top 3 sources are highlighted in bold for each month)*

Site	Type	Biogenic		Biomass		Coal		Diesel		Gas		Industrial		Misc.		Other Comb		Other Mob		Waste		Leftover	
		Jan	Jul	Jan	Jul	Jan	Jul	Jan	Jul	Jan	Jul	Jan	Jul	Jan	Jul	Jan	Jul	Jan	Jul	Jan	Jul	Jan	Jul
JST	Urban	0.8	1.0	**3.4**	0.3	2.3	**7.6**	1.5	**1.3**	**3.9**	**1.7**	1.1	1.1	1.6	0.8	**2.6**	0.8	0.6	0.9	0.2	0.1	0.8	0.1
YRK	Rural	0.8	0.8	**2.3**	0.5	**1.5**	**6.7**	0.4	0.6	0.8	0.5	0.7	**0.8**	**1.9**	**1.4**	0.9	0.5	0.7	0.7	0.1	0.0	0.8	0.1
BHM	Urban	0.7	0.9	1.7	0.3	1.5	**5.6**	0.8	1.0	**1.9**	1.4	**4.9**	**6.7**	1.1	0.5	**2.4**	**1.4**	0.4	0.5	0.2	0.2	0.9	0.5
CTR	Rural	**1.0**	**0.9**	**1.2**	0.2	**1.1**	**3.2**	0.1	0.3	0.3	0.2	0.9	**0.9**	0.7	0.5	0.5	0.4	0.4	0.3	0.0	0.0	1.2	0.6
GFP	Urban	0.4	0.1	**0.6**	0.1	0.5	**1.0**	0.2	0.2	0.3	0.2	**0.6**	**0.7**	0.3	0.1	**0.7**	0.5	0.3	**0.7**	0.0	0.0	2.2	1.2
OAK	Rural	**0.8**	**1.2**	**0.6**	0.2	**0.8**	**1.7**	0.1	0.2	0.2	0.2	0.5	**0.7**	0.5	0.3	0.5	0.4	0.3	0.3	0.0	0.0	1.5	0.7
PNS	Urban	0.2	0.0	**0.8**	0.1	**0.6**	**1.4**	0.1	0.1	0.2	0.1	**0.8**	**0.4**	0.3	0.1	0.5	**0.2**	0.2	0.2	0.0	0.0	2.0	1.6
OLF	Rural	0.5	0.3	**2.6**	0.2	0.7	**1.6**	0.4	0.4	0.7	0.4	**1.4**	**1.0**	0.5	0.3	**1.7**	0.3	0.5	**0.6**	0.0	0.0	1.7	1.2
GRM	Park	0.2	0.3	**2.2**	0.1	**0.8**	**2.9**	0.1	0.3	0.3	0.3	0.3	**0.5**	**0.6**	**0.9**	0.2	0.2	0.2	0.2	0.0	0.0	1.0	3.8
CLT	Urban	0.8	0.7	**3.6**	0.2	**2.3**	**7.9**	1.0	0.9	**2.1**	**1.0**	1.0	0.8	1.7	0.9	1.5	0.5	0.5	**1.2**	0.3	0.2	1.3	0.5
JMS	Rural	1.0	0.3	**2.7**	0.1	**1.9**	**4.0**	0.5	0.3	1.0	0.2	0.8	**0.4**	**3.6**	**1.3**	0.8	0.3	0.3	0.2	0.1	0.0	-0.4	1.6
CHI	Urban	0.3	0.0	1.2	0.0	1.1	**3.8**	1.3	**1.7**	**2.3**	1.1	**3.0**	**4.0**	1.3	0.9	**2.0**	0.8	1.2	1.1	0.8	0.7	3.7	2.6
NYC	Urban	0.6	0.0	**4.9**	0.1	**2.9**	**5.0**	1.8	**2.2**	2.1	1.5	2.6	**2.0**	2.4	1.4	**5.3**	1.4	0.5	0.6	0.4	0.2	4.9	7.2
NOR	Coastal	0.4	0.2	1.1	0.5	0.6	0.9	0.7	0.8	0.5	0.3	**1.8**	**2.5**	**1.2**	0.4	**2.5**	**2.1**	0.6	**1.1**	0.1	0.0	1.9	1.1
CIN	Urban	0.3	0.1	**1.4**	0.2	**1.6**	**9.2**	0.4	0.9	1.0	0.6	1.2	**1.7**	**2.5**	**1.7**	1.0	0.4	0.9	1.3	0.1	0.1	1.9	1.7
KNX	Urban	0.5	0.5	**1.9**	0.5	1.4	**7.3**	0.5	0.6	1.3	0.6	**4.7**	**5.3**	**1.5**	**1.1**	0.7	0.3	0.4	0.6	0.0	0.0	1.3	0.6
NFK	Coastal	0.5	0.0	**1.9**	0.1	**1.9**	**4.2**	0.5	0.5	1.7	0.6	1.1	**0.7**	**1.9**	0.6	1.7	0.5	0.3	**0.7**	0.2	0.1	1.5	3.1
NSH	Urban	0.4	0.0	**1.5**	0.5	**1.4**	**5.7**	0.6	0.7	1.0	0.5	1.3	**1.2**	**1.8**	**1.1**	0.9	0.4	0.6	0.4	0.1	0.0	1.0	0.7

JST: Jefferson Street (Atlanta), GA; YRK: Yorkville, GA; BHML Birmingham, AL; CTR: Centreville, AL; GFP: Gulfport, MS; OAK: Oak Grove, MS; PNS: Pensacola, FL; OLF: Outlying Landing, FL; GRM: Great Smoky Mountain National Park, TN; CLT: Charlotte, NC; JMS: Jamesville, NC; CHI: Chicago, IL; NYC: New York City, NY; NOR: New Orleans, LA; CIN: Cincinnati, OH; KNX: Knoxville, TN; NFK: Norfolk, VA; NSH: Nashville, TN.

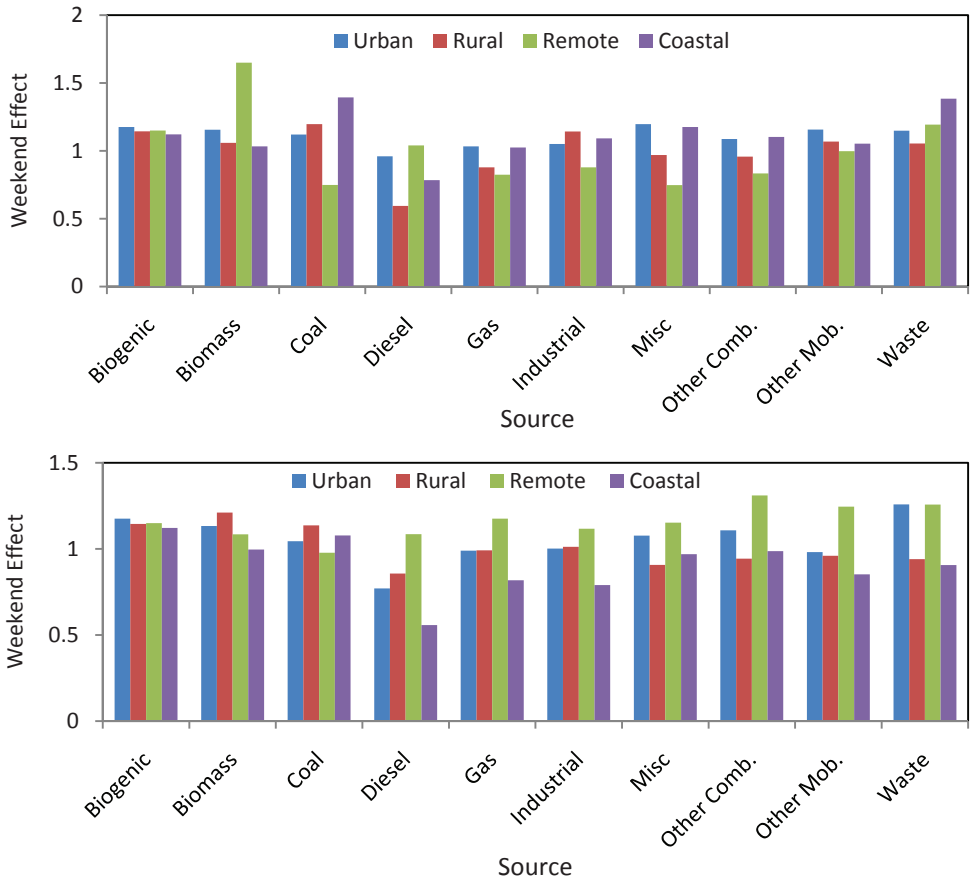

Figure 9. *Weekend effect (defined as the weekend contribution relative to the weekday contribution) for each source category from CMAQ/BFM in January (top) and July (bottom).*

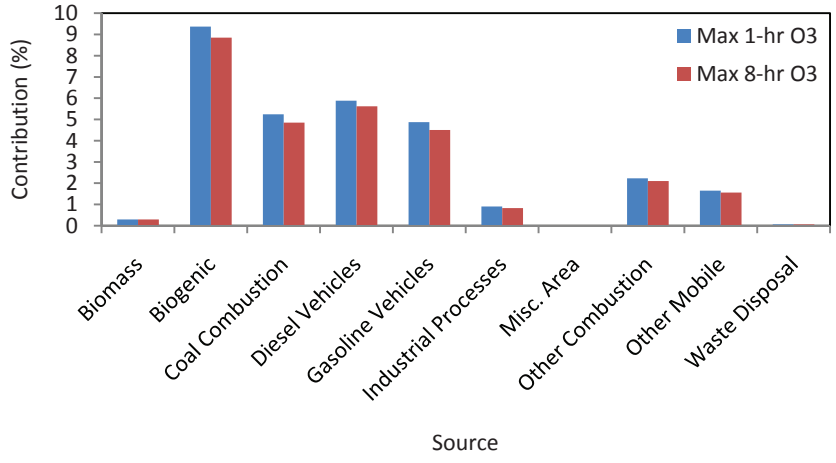

Figure 10. *Source contributions to monthly-mean maximum 1- and 8-h O_3 concentrations in July from CMAQ/BFM.*

sites in July, contributing ~34% and ~39% to monthly–mean $PM_{2.5}$, respectively. Diesel vehicles are found to have the greatest variation in contributions between weekdays and weekends, consistent with previous studies.

Results from this study indicate that coal combustion and biomass burning are two of the most important sources contributing to high $PM_{2.5}$ concentrations in the eastern U.S. In July, SO_4^{2-} formation from coal combustion sources appears to be the most important $PM_{2.5}$ component domainwide. Elimination of coal combustion emissions results in reductions of over 40% of surface monthly–mean $PM_{2.5}$ across much of the domain. While a complete elimination of coal combustions emissions is not a feasible option, adding additional control measures to existing coal–fired power plants may be the most effective method in reducing $PM_{2.5}$ concentrations across the eastern U.S., particularly during the summer months. Control of various biomass burning sources (e.g., prescribed burning, agricultural burning) may be an effective method of reducing $PM_{2.5}$ during the winter months when lower mixing depths result in more build–up of primary PM species. Emissions from gasoline and diesel motor vehicles are also important sources of $PM_{2.5}$, particularly in urban regions where nonattainment is often an issue. These results also indicate that policy–makers must be aware of the effects of reductions in emissions of a certain species on other $PM_{2.5}$ species. For example, large reductions in SO_2 emissions from coal combustion sources

may result in an increase in NO_3^- in some areas. Therefore, combinations of reductions in emissions of several precursor species of secondary PM may be the most effective approach in reducing $PM_{2.5}$ to attainment levels.

While the BFM is advantageous in its relative simplicity and its direct application in the development of emission control measures and its ability to capture indirect effects associated with the interactions of between secondary PM species and their precursors via various pathways, source apportionment results obtained using the BFM are subject to inherent limitations, most notably its assumption that the contributions from each source category are linear and additive. Such an assumption may not be valid for non–linear processes in the atmosphere. In addition, the computational demand of the BFM is usually high when conducting source sensitivity simulations for several source categories. Separate simulations are required for each source category for each month, making the BFM a fairly inefficient approach. In the case of this study, a 1–month simulation for a single source category requires approximately 1.5 hours per simulation day when using 16 processors. As with any emissions–based approach, the accuracy of source apportionment results using the BFM are limited by the ability of the host model to accurately predict the baseline PM concentrations and are subject to uncertainties in the model inputs (i.e., emissions and meteorology) as well as uncertainties in model treatments. For example, model evaluation presented in this study show that $PM_{2.5}$ concentrations are generally overpredicted in January and underpredicted in July, thereby affecting the reliability of the resolved source contributions.

Acknowledgements

This work is supported by the U.S. EPA's Science to Achieve Results (STAR) grant #R833633. We would like to thank Alpine Geophysics, Inc. and the North Carolina Division of Air Quality for providing the emissions inventory and baseline simulation data of which the source apportionment results in this study are based on. Thanks are also due to Xinyi Dong and Kai Wang at NCSU, for their help in post–processing observational data.

Supporting Material Available

Observational dataset used for model evaluation; Model evaluation results; The observational networks and satellites used in model evaluation, as well as the variables evaluated the sampling frequency, and the number of sites within the 12–km domain (Table S1); Performance statistics for surface concentrations of PM components simulated by CMAQ in January 2002 (Table S2); Performance statistics for surface concentrations of PM components simulated by CMAQ in July 2002 (Table S3); Spatial distribution monthly–mean 8–h O_3 and 24–h average $PM_{2.5}$ concentrations simulated by CMAQ overlaid with observations from AIRS–AQS, CASTNET, and SEARCH in January and July (Figure S1). This information is available free of charge via the Internet at http://www.atmospolres.com.

References

Baker, K., Timin, B., 2008. $PM_{2.5}$ source apportionment comparison of CMAQ and CAMX estimates. *Presented at the 7th Annual Community Modeling and Analysis System (CMAS) Conference*, Chapel Hill, October 6-8, 2008, N.C.

Barnard, W.R., Sabo, E., 2008. Documentation of the Base G2 and Best and Final 2002 Base Year, 2009 and 2018 Emission Inventories for VISTAS, MACTEC Engineering and Consulting, Inc. Prepared for the Visibility Improvement State and Tribal Association of the Southeast (VISTAS), March 14.

Bhave, P.V., Pouliot, G.A., Zheng, M., 2007. Diagnostic model evaluation for carbonaceous $PM_{2.5}$ using organic markers measured in the southeastern U.S. *Environmental Science and Technology* 41, 1577-1583.

Burr, M., Zhang, Y., 2011. Source apportionment of fine particulate matter over the Eastern U.S. Part II: Source apportionment simulations using CAMx/PSAT and comparisons with CMAQ source sensitivity simulations. *Atmospheric Pollution Research* 2, 317-335.

Byun, D., Schere, K.L., 2006. Review of the governing equations, computational algorithms, and other components of the Models-3 Community Multiscale Air Quality (CMAQ) modeling system. *Applied Mechanics Reviews* 59, 51-77.

Dunker, A.M., 1984. The decoupled direct method for calculating sensitivity coefficients in chemical kinetics. *Journal of Chemical Physics* 81, 2385-2393.

Eder, B., Yu, S.C., 2006. A performance evaluation of the 2004 release of Models-3 CMAQ. *Atmospheric Environment* 40, 4811-4824.

EIP, 2007. Dirty Kilowatts, America's Most Polluting Power Plants, The Environmental Integrity Project (EIP) report, EIP, Washington, DC 20036, July, also see http://www.dirtykilowatts.org/index.cfm.

Grell, G.A., Dudhia, J., Stauffer, D.R., 1995. A description of the Fifth-Generation Penn State/NCAR Mesoscale Model (MM5). NCAR Technical Report, NCAR/TN-398+STR, 122.

Hakami, A., Odman, M.T., Russell, A.G., 2004. Nonlinearity in atmospheric response: a direct sensitivity analysis approach. *Journal of Geophysical Research-Atmospheres* 109, art. no. D15303.

Hopke, P.K., 1991. *Receptor Modeling for Air Quality Management*. Elsevier Science, Amsterdam.

Hwang, I., Hopke, P.K., 2007. Estimation of source apportionment and potential source locations of $PM_{2.5}$ at a west coastal IMPROVE site. *Atmospheric Environment* 41, 506-518.

Ke, L., Liu, W., Wang, Y., Russell, A.G., Edgerton, E.S., Zheng, M., 2008. Comparison of $PM_{2.5}$ source apportionment using positive matrix factorization and molecular marker-based chemical mass balance. *Science of the Total Environment* 394, 290-302.

Koo, B., Wilson, G.M., Morris, R.E., Dunker, A.M., Yarwood, G., 2009. Comparison of source apportionment and sensitivity analysis in a particulate matter air quality model. *Environmental Science and Technology* 43, 6669-6675.

Laden, F., Neas, L.M., Dockery, D.W., Schwartz, J., 2000. Association of fine particulate matter from different sources with daily mortality in six U.S. Cities. *Environmental Health Perspectives* 108, 941-947.

Lall, R., Thurston, G.D., 2006. Identifying and quantifying transported vs. Local sources of New York City $PM_{2.5}$ fine particulate matter air pollution. *Atmospheric Environment* 40, 333-346.

Lee, D., Balachandran, S., Pachon, J., Shankaran, R., Lee, S., Mulholland, J.A., Russell, A.G., 2009. Ensemble-trained $PM_{2.5}$ source apportionment approach for health studies. *Environmental Science and Technology* 43, 7023-7031.

Liu, X.H., Zhang, Y., Olsen, K.M., Wang, W.X., Do, B.A., Bridgers, G.M., 2010a. Responses of future air quality to emission controls over North Carolina, Part I: Model evaluation for current year simulations. *Atmospheric Environment* 44, 2443-2456.

Liu, X.H., Zhang, Y., Xing, J., Zhang, Q.A., Wang, K., Streets, D.G., Jang, C., Wang, W.X., Hao, J.M., 2010b. Understanding of regional air pollution over China using CMAQ, Part II. Process analysis and sensitivity of ozone and particulate matter to precursor emissions. *Atmospheric Environment* 44, 3719-3727.

Marmur, A., Unal, A., Mulholland, J.A., Russell, A.G., 2005. Optimization based source apportionment of $PM_{2.5}$ incorporating gas-to-particle ratios. *Environmental Science and Technology* 39, 3245-3254.

Meng, Z., Dabdub, D., Seinfeld, J.H., 1997. Chemical coupling between atmospheric ozone and particulate matter. *Science* 277, 116-119.

Morris, R.E., Koo, B., Piyachaturawat, P., Stella, G., McNally, D., Loomis, C., Chien, C.-J., Tonnesen G., 2009. Technical Support Document for VISTAS Emissions and Air Quality Modeling to Support Regional Haze State Implementation Plans. Final Report, ENVIRON, Novata, CA.

Olerud, D., Sims, A., 2004. MM5 2002 modeling in support of VISTAS (Visibility Improvement – State and Tribal Association of the Southeast), Baron Advanced Meteorological Systems, LLC, Raleigh, NC.

Olsen, K.M., 2009. *Fine Scale Modeling of Agricultural Air Quality over The Southeastern United States: Application and Evaluation of Two Air Quality Models*. MS Thesis, North Carolina State University, Raleigh, NC.

Pai, P., Vijayaraghavan, K., Seigneur, C., 2000. Particulate matter modeling in the Los Angeles Basin using SAQM-AERO. *Journal of the Air and Waste Management Association* 50, 32-42.

Pun, B.K., Seigneur, C., Bailey, E.M., Gautney, L.L., Douglas, S.G., Haney, J.L., Kumar, N., 2008. Response of atmospheric particulate matter to changes in precursor emissions: a comparison of three air quality models. *Environmental Science and Technology* 42, 831-837.

Seigneur, C., Pai, P., Hopke, P.K., Grosjean, D., 1999. Modeling atmospheric: particulate matter. *Environmental Science and Technology* 33, 80A-86A.

Tian, D., Hu, Y.T., Wang, Y.H., Boylan, J.W., Zheng, M., Russell, A.G., 2009. Assessment of biomass burning emissions and their impacts on urban and regional $PM_{2.5}$: a Georgia case study. *Environmental Science and Technology* 43, 299-305.

Wagstrom, K.M., Pandis, S.N., Yarwood, G., Wilson, G.M., Morris, R.E., 2008. Development and application of a computationally efficient particulate matter apportionment algorithm in a three-dimensional chemical transport model. *Atmospheric Environment* 42, 5650-5659.

Wang, Z.S., Chien, C.J., Tonnesen, G.S., 2009. Development of a tagged species source apportionment algorithm to characterize three-dimensional transport and transformation of precursors and secondary pollutants. *Journal of Geophysical Research-Atmospheres* 114, art. no. D21206.

Watson, J.G., 1984. Overview of receptor model principles. *Journal of the Air Pollution Control Association* 34, 619-623.

Yarwood, G., Wilson, G., Morris, R., 2005. Development of the CAMx Particulate Source Apportionment Technology (PSAT), Final Report, ENVIRON International Corporation, Prepared for Lake Michigan Air Directors Consortium, Novato, CA.

Zhang, Y., Vijayaraghavan, K., Wen, X.Y., Snell, H.E., Jacobson, M.Z., 2009. Probing into regional ozone and particulate matter pollution in the United States: 1. A 1 year CMAQ simulation and evaluation using surface and satellite data. *Journal of Geophysical Research-Atmospheres* 114, art. no. D22304.

Zhang, Y., Liu, P., Pun, B., Seigneur, C., 2006a. A comprehensive performance evaluation of MM5-CMAQ for the summer 1999 southern Oxidants Study Episode, Part I: Evaluation protocols, databases and meteorological predictions. *Atmospheric Environment* 40, 4825-4838.

Zhang, Y., Liu, P., Queen, A., Misenis, C., Pun, B., Seigneur, C., Wu, S.Y., 2006b. A comprehensive performance evaluation of MM5-CMAQ for the summer 1999 southern oxidants study episode, Part II: Gas and aerosol predictions. *Atmospheric Environment* 40, 4839-4855.

Zhang, Y., Vijayaraghavan, K., Seigneur, C., 2005. Evaluation of three probing techniques in a three-dimensional air quality model. *Journal of Geophysical Research-Atmospheres* 110, art. no. D02305.

Zheng, M., Ke, L., Edgerton, E.S., Schauer, J.J., Dong, M.Y., Russell, A.G., 2006. Spatial distribution of carbonaceous aerosol in the Southeastern United States using molecular markers and carbon isotope data. *Journal of Geophysical Research-Atmospheres* 111, art. no. D10S06.

Zheng, M., Cass, G.R., Schauer, J.J., Edgerton, E.S., 2002. Source apportionment of $PM_{2.5}$ in the Southeastern United States using solvent-extractable organic compounds as tracers. *Environmental Science and Technology* 36, 2361-2371.